

**MERLIN RELATION TO CELL STRUCTURE AND ADHESION  
IN NA,K-ATPASE  $\beta_2$  DEFICIENT CEREBELLAR NEURON PROGENITORS**

by

Patience Kelly

A thesis submitted to the Faculty of the University of Delaware in partial fulfillment of the requirements for the degree of Master of Science in Biological Sciences

Fall 2019

© 2019 Patience Kelly  
All Rights Reserved

**MERLIN RELATION TO CELL STRUCTURE AND ADHESION  
IN NA,K-ATPASE  $\beta_2$  DEFICIENT CEREBELLAR NEURON PROGENITORS**

by

Patience Kelly

Approved: \_\_\_\_\_  
Erica Selva, Ph.D.  
Co-professor in charge of thesis on behalf of the Advisory Committee

Approved: \_\_\_\_\_  
Sigrid Langhans, Ph.D.  
Co-professor in charge of thesis on behalf of the Advisory Committee

Approved: \_\_\_\_\_  
Velia Fowler, Ph.D  
Chair of the Department of Biological Sciences

Approved: \_\_\_\_\_  
John A. Pelesko, Ph.D.  
Dean of the College of Arts and Sciences

Approved: \_\_\_\_\_  
Douglas J. Doren, Ph.D.  
Interim Vice Provost for Graduate and Professional Education and  
Dean of the Graduate College

## ACKNOWLEDGMENTS

I would first like to thank my advisor, Dr. Sigrid Langhans, for allowing me to join her lab with my limited experience. Her support, understanding, and guidance made my time at Nemours the least stressful and most peaceful it could be. Thank you to Dr. Erica Selva and Dr. Donna Woulfe, my committee members, who have offered great support and advice throughout the past two years. I am also really grateful to Dr. Zhiqin Li, our lab's postdoc, for all of her instructions, moral support, and help with troubleshooting. Thank you to Alisa, who continued to answer questions and help me with protocols and methods even after graduating.

A big thank you to Ellen Hitchens, April and the Life Science Center staff, and to Terry and the Histochemistry and Tissue Processing Core staff. Without them, my work would have been twice as difficult and time-consuming. Thank you also to Karen Sperle and SNERPs for their technical and personal advice. I would also like to thank the Nemours Foundation and the University of Delaware for my funding, including the Grad Scholars Award.

Moving halfway across the country to pursue a graduate degree was quite the experience, so I would like to thank my family, Anil, Danielle, my AP church family, and my friends for all the love and support they gave me these past two years. Thank you for encouraging me, visiting, and sending gifts, I appreciate everything and hope I make you proud. I also thank God, the reason I am constantly in awe of life – from the molecular to the environmental, and decided to the reason that I could work with excitement and love, in spite of frustrations and setbacks.

## TABLE OF CONTENTS

LIST OF FIGURES .....	vi
ABSTRACT .....	viii
Chapter	
1 INTRODUCTION .....	1
1.1 Na,K-ATPase $\beta_2$ .....	1
1.1.1 Na,K-ATPase Isoform Specificity .....	2
2 MERLIN .....	6
2.1 Introduction .....	6
2.2 Merlin and Cellular Signaling .....	7
2.3 Merlin and Focal Adhesions .....	8
2.4 Merlin and EGFR .....	9
2.5 $\beta_2$ and Merlin .....	10
2.6 Hypothesis and Aims .....	10
3 METHODS .....	12
3.1 Animals .....	12
3.2 Cell Culture .....	12
3.3 Antibodies .....	13
3.4 Immunoblot .....	13
3.5 Coimmunoprecipitation .....	14
3.6 Immunofluorescence .....	15
3.7 Immunohistology .....	15
3.8 Merlin Double Knockdown .....	16
4 RESULTS .....	17
4.1 Postnatal Expression of Merlin and Associated Proteins .....	17
4.2 Protein Localization .....	18
4.2.1 Merlin and Actin .....	19
4.2.2 Merlin and EGFR .....	21
4.2.3 Merlin and Focal Adhesion Proteins .....	24
4.2.4 Merlin and Phospho-YAP .....	26
4.2.5 Summary of Localization Results .....	26

4.3	Coimmunoprecipitation.....	32
4.4	Merlin Knockdown.....	33
4.5	Immunohistochemistry .....	34
5	DISCUSSION.....	37
5.1	Merlin and Focal Adhesion Proteins .....	37
5.2	Future Directions and Considerations .....	39
	REFERENCES .....	42
Appendix		
A	SUPPLEMENTARY IMAGES.....	46
B	WT AND AMOG <sup>-/-</sup> CEREBELLAR MORPHOLOGY .....	48
C	PRIMARY CELL CULTURE .....	49
D	BETA KNOCKDOWN MEDULLOSPHERES .....	51

## LIST OF FIGURES

Figure 1. Na,K-ATPase subunit and Merlin expression in mouse cerebellum .....	3
Figure 2. Phenotypes of $\beta_2$ knockdown in DAOY cells.....	4
Figure 3. Postnatal expression of phosphorylated signaling proteins in WT and AMOG <sup>-/-</sup> cerebellar tissue .....	18
Figure 4. Postnatal $\beta_2$ , Merlin, and focal adhesion proteins expression in cerebellar tissue.....	18
Figure 5. Merlin and actin localization in $\beta_2$ knockdown cells .....	20
Figure 6. Merlin and actin localization in $\beta_1$ knockdown cells .....	22
Figure 7. Merlin and EGFR localization in $\beta_2$ knockdown cells.....	23
Figure 8. Merlin and vinculin localization in $\beta_2$ knockdown cells.....	25
Figure 9. Merlin and vinculin in $\beta_1$ knockdown cells.....	27
Figure 10. Merlin and paxillin localization in $\beta_2$ knockdown cells.....	28
Figure 11. Merlin and paxillin in $\beta_1$ knockdown cells.....	29
Figure 12. Merlin and phospho-FAK localization in $\beta_2$ knockdown cells.....	30
Figure 13. Merlin and phospho-YAP localization in $\beta_2$ knockdown cells.....	31
Figure 14. Coimmunoprecipitation targeting Merlin-associated proteins in WT cerebellum .....	32
Figure 15. Merlin knockdown in $\beta_2$ knockdown cells.....	33
Figure 16. Merlin and actin in postnatal WT and AMOG <sup>-/-</sup> cerebellar tissue.....	34
Figure 17. Merlin and EGFR in postnatal WT and AMOG <sup>-/-</sup> cerebellar tissue .....	35
Figure A1. $\beta_2$ knockdown cells primary control .....	46
Figure A2. $\beta_1$ knockdown cells primary control .....	47
Figure B1. Tissue morphology of WT and AMOG <sup>-/-</sup> cerebellar tissue .....	48
Figure C1. Actin in cerebellar granule progenitor cells .....	49

Figure C2. Acetylated $\alpha$ -tubulin in cerebellar granule progenitor cells .....	50
Figure D1. Medullosphere culture of $\beta$ KD cells .....	51

## ABSTRACT

The Na,K-ATPase is an ion pump that contains a catalytic  $\alpha$  subunit, a glycosylated  $\beta$  subunit, and an auxiliary  $\gamma$  subunit. The  $\beta$  subunits are necessary for sorting the Na,K-ATPase to the cell membrane and are involved in cell adhesion. Out of the three  $\beta$  isoforms ( $\beta_1$ ,  $\beta_2$  or AMOG,  $\beta_3$ ),  $\beta_1$  and  $\beta_2$  are expressed in cerebellar granule cells, but their differences in glycosylation and low sequence identity suggests isoform-specific functions. In medulloblastoma cells, knockdown of  $\beta_2$  has a greater effect on Na,K-ATPase pump activity and in cerebellar granule cell progenitors,  $\beta_2$  expression is less affected by Sonic Hedgehog signaling activation than  $\beta_1$  expression.  $\beta_2$  knockdown cells have a more rounded morphology and prolonged Epidermal Growth Factor Receptor (EGFR) activation. These findings may be related to the concurrent increase in Merlin, a linker protein that connects membrane proteins to the cytoskeleton that is associated with EGFR internalization, focal adhesions, and cell junctions. To further investigate Merlin's neuronal function and interactions in the absence of  $\beta_2$ , the localization and expression of focal adhesion proteins and actin were assessed in DAOY cells and cerebellar tissue. Merlin was mostly cytoplasmic but intermittently overlapped with EGFR, focal adhesion proteins vinculin and paxillin at the membrane of  $\beta_2$  knockdown cells. EGFR was internalized when cells were treated with EGF, with differences in endosomal localization in  $\beta_2$  knockdown cells. Protein expression of focal adhesion proteins in  $\beta_2$  knockout (AMOG<sup>-/-</sup>) cerebellar tissue was similar to wild-type postnatally, while Merlin expression increases in AMOG<sup>-/-</sup> cerebellum.

## Chapter 1

### INTRODUCTION

#### 1.1 Na,K-ATPase $\beta_2$

The Na,K-ATPase is an ATP-dependent ion pump that exchanges 3 Na<sup>+</sup> for 2 K<sup>+</sup>, which creates an efflux of sodium and an influx of potassium thereby generating an electrochemical gradient across the membrane (1,2). This maintains the ion homeostasis of the cell and is crucial for generating action potentials and metabolism. The Na,K-ATPase is expressed in all cell types and is involved in the regulation of cell volume, polarity, and motility (3-6). The cardiotonic steroid ouabain binds to the Na,K-ATPase and, depending on its concentration, inhibits pump function or induces signaling (7,8). There are several signaling pathways where Na,K-ATPase is indirectly involved as a scaffold for signaling proteins, including the Ras, phosphoinositide 3-kinase (PI3K), and Src signaling pathways (9-11).

In epithelial cells, the Na,K-ATPase may act as a signaling hub at cell junction complexes, where  $\beta_1$  functions as an adhesion molecule (12).  $\beta_2$  is also an adhesion molecule, as it was first discovered as a glycoprotein necessary for neuron migration along glia and named AMOG (Adhesion Molecule on Glia) (13). Extensive research on the Na,K-ATPase has been conducted mostly in epithelial cells, comparatively little is known about  $\beta_2$  and its role in cell-cell contact in the brain. This is particularly interesting given the importance of the Na,K-ATPase in regulating ion flux, depolarization, and the unique interaction of glial and neuronal cells.

### 1.1.1 Na,K-ATPase Isoform Specificity

Na,K-ATPase consists of three subunits:  $\alpha$ ,  $\beta$ , and  $\gamma$ . The  $\alpha$  subunit ( $\alpha_1$ ,  $\alpha_2$ ,  $\alpha_3$ ,  $\alpha_4$ ) exchanges three sodium ions for two potassium ions, while the glycosylated  $\beta$  subunit ( $\beta_1$ ,  $\beta_2$ ,  $\beta_3$ ) targets the protein to the cell membrane where isoforms  $\beta_1$  and  $\beta_2$  serve as cell adhesion molecules (1). The regulatory  $\gamma$  subunit belongs to the FXYD family of proteins. Na,K-ATPase isoforms are usually expressed in specific combinations of  $\alpha$  and  $\beta$  in different tissues, with  $\alpha_1\beta_1$  being the most common (1). There is a range in  $\text{Na}^+$  affinity and pump catalytic activity between isoforms, likely due to the slight differences in tilt angle of the  $\beta$  subunit (3,14). In the brain,  $\alpha_1$  and  $\beta_1$  are the housekeeping isoforms, expressed in both neurons and glial cells, while  $\alpha_2$  and  $\beta_2$  expression is higher in astrocytes (3). Both  $\beta_1$  and  $\beta_2$  isoforms are expressed in cerebellar granule progenitor (CGP) cells in the cerebellum (15).

The  $\beta$  isoforms are particularly interesting due to their relatively low percentage of sequence identity. There is only 39% sequence identity between  $\beta_1$  and  $\beta_2$ , suggesting different functions for the two isoforms (16,17). Both  $\beta_1$  and  $\beta_2$  are glycosylated and important in cell-cell adhesion, but there is a stark difference in number of glycosylation sites and evidence that  $\beta_2$  has functions that cannot be completely compensated for by the substitution of  $\beta_1$  (18,19).  $\beta_2$  has at least seven N-linked glycosylation sites compared to the three  $\beta_1$  sites which are necessary for homotypic dimerization (19,20). Homotypic trans-dimerization of the  $\beta_1$  subunit is directly related to adherens junction stability in epithelial cells (21). There has not been consistent research on  $\beta_2$  over the years and it is unknown whether similar findings also apply to neuronal cells.

Early on, Magyar et al. bred a strain of  $\beta_2$  knockout mice ( $\text{AMOG}^{-/-}$ ) and found that these mice display motor incoordination and tremors around P15 and die 17 – 18

days after birth (18). Little is known about  $\beta_2$ /AMOG's role in neurons other than its importance in neuron-astrocyte adhesion (13,16). In comparison, the  $\beta_1$  subunit is well-studied as a component of cell junctions in epithelial cells (7,12,22) and has been shown to be regulated by Sonic Hedgehog (SHH) signaling in CGP cells (4). Granule cells are the most numerous type of neurons in the brain and during cerebellar development, the proliferation of granule progenitor cells is triggered by SHH (23,24). Litan et al. showed that after treating primary CGP cells with SAG, a SHH signaling agonist,  $\beta_1$  expression is reduced to a greater degree than  $\beta_2$  expression (Fig. 1C) (17). This was another indication, in addition to sequence and glycosylation differences, that  $\beta_2$  may have other or additional isoform-specific functions.

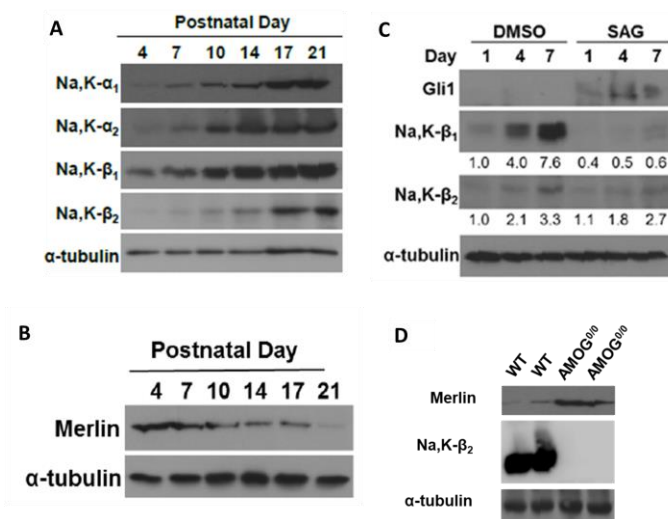


Figure 1. Na,K-ATPase subunit and Merlin expression in mouse cerebellum. A, B, Merlin and  $\beta_1/\beta_2$  are inversely related in WT cerebellum. C, SHH signaling has a greater effect on  $\beta_1$  expression in SAG treated CGP cells. D, Merlin expression in  $\beta_2$  knockout (AMOG<sup>-/-</sup>) cerebellum (17).

To further study the functions of  $\beta_1$  and  $\beta_2$ , our lab generated knockdown cell lines using DAOY cells (Fig. 2A) (17,22). When  $\beta_1$  was knocked down in DAOY cells, a human medulloblastoma-derived cell line, proliferation increased. However, when  $\beta_2$  was knocked down, there were no significant changes in proliferation. In terms of cell-cell contact,  $\beta_2$  knockdown decreased cell aggregation compared to  $\beta_1$  knockdown, suggesting that  $\beta_2$  may have a greater impact on cell-cell adhesion than  $\beta_1$  (25). Pump activity of the  $\alpha$  subunit was also more affected by  $\beta_2$  knockdown than by  $\beta_1$  knockdown in DAOY cells (Fig. 2B) (14,17). When induced with epidermal growth factor,  $\beta_2$  knockdown cells had a circumferential actin ring and abnormal formation of

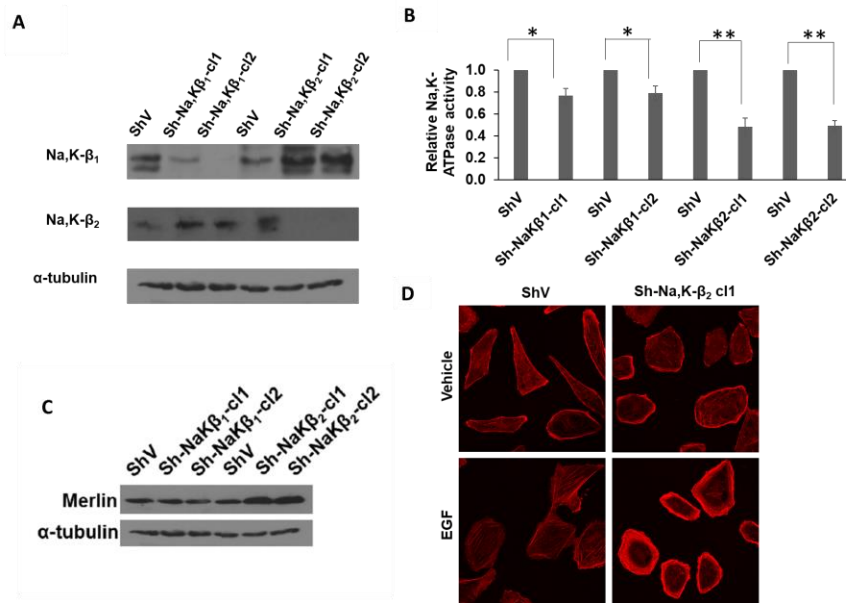


Figure 2. Phenotypes of  $\beta_2$  knockdown in DAOY cells. A, Stable  $\beta_1$  and  $\beta_2$  knockdown cell lines were previously created in our lab. B,  $\beta_2$  KD in DAOY cells has a greater effect on pump activity. C, Merlin increases in  $\beta_2$  KD cells. D, epidermal growth factor (EGF) treated  $\beta_2$  cells have a cortical actin ring and more rounded morphology (17).

stress fibers (Fig. 2D) (17). These findings prompted questions about what other factors were involved in these phenotypes which somehow link the Epidermal Growth Factor Receptor (EGFR), actin structure, cell adhesion, and  $\beta_2$  together.

Merlin (Moesin-Ezrin-Radixin-Like Protein) was identified as a possible mediator between  $\beta_2$  adhesion function and cytoskeletal changes seen in  $\beta_2$  knockdown cells. While  $\beta_2$  increases after P4 in wild-type (WT) mouse cerebellum, Merlin expression decreases postnatally (Fig. 1B) and is elevated in AMOG<sup>-/-</sup> cerebellum and  $\beta_2$  knockdown cells (Fig. 1D, 2C) (17). Considering the inverse relationship of  $\beta_2$  and Merlin expression at both the RNA and protein level, direct contact between the two may not be likely. To better understand the phenotypes caused by  $\beta_2$  knockdown, the goal of this study was to characterize Merlin expression and determine what other proteins it may be working with in our cell lines and cerebellar tissue.

## Chapter 2

### MERLIN

#### 2.1 Introduction

Neurofibromin 2, or Merlin (Moesin-Ezrin-Radixin-Like Protein), is a tumor suppressor protein that links the cytoskeleton to membrane proteins (26). Inactivating mutations of the *NF2* gene cause neurofibromatosis type 2 (NF2), an inherited autosomal disease characterized by bilateral vestibular schwannomas, loss of hearing, and neuropathy (27). Compared to other members of the 4.1 family of ERM (Ezrin, Radixin, Moesin) proteins, Merlin has a distinctive role as a tumor suppressor (28). Merlin and the ERM proteins are made of a N-terminal FERM (band 4.1 protein ezrin-radixin-moesin) domain that binds to membrane proteins, a coiled coil, and a C-terminal domain that connect lipids and membrane proteins to the cytoskeleton (29). This allows for external information about the cell's environment to be transmitted to proteins inside the cell, which is important for processes like cell growth and migration.

Due to its disease-causing role in NF2, previous Merlin research has mostly focused on the peripheral nervous system and glial cells. Although less characterized, Merlin also has neuron-specific functions. In oligodendrocytes, cerebellar granule cells, and Purkinje cells, Merlin inhibits neurite outgrowth (30-32). These findings suggest that Merlin can inhibit differentiation, which could be directly related to the postnatal decrease in Merlin seen in WT cerebellum (17). Just as research on  $\beta_2$  is lacking, research on Merlin's role in neurons is also lacking. To better understand the two and what they contribute to cell adhesion and intracellular signaling in neurons,

this study assessed Merlin's relationship to focal adhesions, actin organization, and EGFR signaling.

## **2.2 Merlin and Cellular Signaling**

There are several signaling pathways and kinases that are affected by Merlin, such as Rac1-PAK (Rac family small GTPase 1, protein A kinase), phosphoinositide 3-kinase (PI3K), and epidermal growth factor receptor (EGFR) signaling (32-35). In glial cells, Merlin knockout resulted in an increase in phospho-Src and phospho-ErbB2, which are related to differentiation, proliferation, and motility (36). These processes require reorganization of filaments and microtubules. Merlin directly binds actin and regulates  $\alpha$ -tubulin polymerization, mediating the coordination of cytoskeletal dynamics and extracellular stimuli (37,38). Work from our lab has shown that knockdown of  $\beta_2$  in DAOY cells results in higher levels of Merlin expression and disorganization of the actin cytoskeleton (17). To uncover more of Merlin's implications in  $\beta_2$  knockdown and AMOG<sup>-/-</sup> mice, analysis of signaling pathways that use both the Na,K-ATPase and Merlin as scaffolds may provide useful information about cellular changes during migration, differentiation, and growth.

One of the Merlin-inhibited signaling pathways is the Hippo-YAP signaling pathway, which regulates organ growth and prevents tumorigenesis. Merlin has been shown to regulate the activation of YAP, preventing the transcription of genes involved in expanding cell size (39). Merlin acts as a scaffold and activator for downstream proteins such as LATS1/2, which phosphorylates YAP and prevents its translocation to the nucleus (39). Our lab previously found that YAP inactivation increased in clones of  $\beta_2$  knockdown cells, and this increase in p-YAP is not a result of attenuated pump activity. However, the localization of endogenous Merlin and YAP

localization remains to be determined in these  $\beta_2$  knockdown cells and the developing cerebellum.

### **2.3 Merlin and Focal Adhesions**

While much remains unknown about Merlin's effects on neuron progenitors in the central nervous system, many studies have focused on its functions in the peripheral nervous system. Endogenous Merlin expression in neuronal cells is mostly cytoplasmic and localizes to cell membrane structures in glial cells, along with actin and focal adhesion proteins, like paxillin (31,40). Src forms a complex with paxillin and focal adhesion kinase (FAK), and all three proteins are phosphorylated and activated in  $NF2^{-/-}$  glia, indicating that Src signaling and activation of focal adhesion proteins are Merlin-dependent (36,41,42). This is supported by preliminary data from our lab showing a slight increase in FAK inactivation in  $\beta_2$  knockdown cells, which was reversed by  $\beta_2$  rescue and by Merlin knockdown (Litan, unpublished data). In malignant mesothelioma cells, Merlin also negatively regulated the phosphorylation and activation of FAK, inhibiting the downstream PI3K signaling cascade (43).

As for paxillin, it directly binds Merlin, as shown in Schwann cells, and localizes to points of cell-cell contact, filopodia, and membrane ruffles (40). The focal adhesion scaffold protein vinculin also binds paxillin and, in  $NF2^{-/-}$  epithelial cells, vinculin expression at adherens junctions increases (44). These findings collectively support Merlin's role as an inhibitor of migration and proliferation-related pathways in different cell types, but Merlin's relation to these proteins has yet to be confirmed in neurons of the central nervous system.

## 2.4 Merlin and EGFR

In addition to its interaction with focal adhesion and cytoskeletal components, Merlin is known to regulate EGFR signaling (33,44). Merlin expression prevents both EGFR internalization and the movement of EGFR within the plasma membrane (44). EGFR activation is also inhibited by Merlin expression, possibly providing a link between actin organization, growth signaling, and cell-cell contact, especially when EGF's induction of actin stress fibers is taken into account (45). In  $\beta_2$  knockdown ( $\beta_2$  KD) cells, Merlin expression is higher and EGFR activation is increased and sustained, compared to vector control cells (17). Canonical EGFR signaling is not affected by  $\beta_2$  knockdown and these effects on EGFR activation can be reversed by Merlin knockdown or  $\beta_2$  rescue. The spatial relationship between Merlin and EGFR in  $\beta_2$  KD cells has not been analyzed yet. Whether these findings apply to the *in vivo* processes of granule progenitor cell proliferation and differentiation during cerebellar development is not yet known.

Previously, Litan et al. found that Merlin decreases postnatally in WT cerebellum, which is inversely related to the increase in expression of Na,K-ATPase subunit  $\beta_2$  (17). Merlin expression was also higher in AMOG<sup>-/-</sup> mice. Although we know EGFR activation is prolonged in  $\beta_2$  knockdown cells, *in vivo* EGFR expression and activation in AMOG<sup>-/-</sup> cerebellum has not been studied. As an inhibitor of cell spreading, proliferation, and invasion, Merlin could be contributing to changes in EGFR activation when  $\beta_2$  is absent or deficient, but more *in vitro* and *in vivo* work is necessary to confirm this hypothesis.

## 2.5 $\beta_2$ and Merlin

Merlin is upregulated in  $\beta_2$  knockdown cells and in AMOG<sup>-/-</sup> cerebellum. Merlin has been described as a tumor suppressor and scaffold protein and shares a few cellular functions with  $\beta_2$ . Both  $\beta_2$  and Merlin deficiency can cause actin disorganization (17,46). Based on the effects Merlin and  $\beta_2$  have on actin and EGFR signaling, both proteins contribute to cell motility and signaling. At the extracellular level,  $\beta_2$  acts as an adhesion molecule. At the membrane level, it affects the K<sup>+</sup> affinity of the  $\alpha$  subunit. Merlin, on the other hand, operates in the cytoplasm and cell cortex. Both the Na,K-ATPase and Merlin act as scaffolds for signaling and actin. Although they may not interact directly, it is possible that higher Merlin expression in  $\beta_2$  knockdown cells could be a response to reduced cell adhesion.

## 2.6 Hypothesis and Aims

Merlin, an important regulator of neuronal growth and migration, is implicated in the effects of  $\beta_2$  knockdown on EGFR signaling and actin organization in medulloblastoma cells (17). Both Merlin and Na,K-ATPase are also involved in PI3K and EGFR signaling, as a hub for signaling (9,43,46). Loss of  $\beta_2$  leads to less cell-cell contact and aggregation, indicating that the increase in Merlin expression compensates at the subcortical level for the loss of adhesion (Litan, unpublished data). The question to be addressed in this thesis is whether Merlin associates with focal adhesion proteins, EGFR, and structural proteins in DAOY cells and CGP cells, and whether those associations are affected by  $\beta_2$  expression.

I hypothesize that Merlin's distribution in the cell will overlap with that of actin, EGFR, and focal adhesion proteins at the cell membrane, and this localization will be more prominent in  $\beta_2$  knockdown cells where Merlin expression is higher. In

cells induced to migrate with EGF, I hypothesize that Merlin and focal adhesion proteins will localize to both the leading and trailing edges of the cell as cell-surface adhesion sites change. Merlin and actin colocalization is expected to be more obvious in EGF-treated cells, as Merlin regulates actin dynamics. As for Merlin's role in EGF and Hippo signaling, I hypothesize that Merlin will not be internalized with EGFR in EGF-treated cells, and that cytosolic p-YAP will be more prominent in  $\beta_2$  knockdown cells. Effects of  $\beta_2$  knockdown on EGFR signaling are not expected to be visible in studies of localization. In the cerebellum, I hypothesize that Merlin expression will increase in AMOG<sup>-/-</sup> mice, and that YAP inactivation will be higher, while EGFR and FAK activation will increase along with paxillin expression.

Merlin will increase that Since Merlin expression has been shown to increase in  $\beta_2$  knockdown cells and tissue, this study aimed to address three points. First, the protein expression levels of proteins known to interact with Merlin, such as FAK, paxillin, and vinculin, in wild-type and AMOG<sup>-/-</sup> cerebella were analyzed through western blotting. Second, the localization of focal adhesion proteins associated with Merlin was determined in  $\beta_2$  knockdown cells through immunofluorescence. Third, confirmation of Merlin association with focal adhesion proteins was evaluated in WT tissue through coimmunoprecipitation.

## Chapter 3

### METHODS

#### 3.1 Animals

All animals were housed and handled in accordance with IACUC regulations. AMOG<sup>+/-</sup> were bred and genotyped to collect postnatal tissue from WT and AMOG<sup>-/-</sup> littermates. C57Bl6/J mice were used to generate cerebellar primary cultures. Pups older than P10 were euthanized with CO<sub>2</sub> followed by decapitation or cervical dislocation. Before P10, pups were euthanized via decapitation.

#### 3.2 Cell Culture

DAOY knockdown cell lines (ShV Cl. 1, Sh $\beta_2$  Cl. 1, ShV Cl. 3, Sh $\beta_1$  Cl. 3) were maintained with Eagle's minimum essential medium, supplemented with 10% fetal bovine serum and 1% gentamicin-penicillin-streptavidin. Sh $\beta_2$  Cl. 1 and ShV Cl. 1 are the  $\beta_2$  knockdown ( $\beta_2$  KD) and vector control medulloblastoma cell lines, while Sh $\beta_1$  Cl. 3 and ShV Cl. 3 are the  $\beta_1$  knockdown ( $\beta_1$  KD) and scrambled shRNA control medulloblastoma cell lines, respectively. Stable cell lines used in these experiments were previously created using shRNA knockdown with an empty pSIREN-DNR-DsRed-Express (Clontech, Mountain View, CA) vector (ShV Cl. 1) or scrambled vector, for ShV Cl. 3 (5'-GTGATGCTGCTCACCATCA-3'), in the pSilencer 5.1 vector (Ambion, Austin, TX) in DAOY cells (17,22). The Sh $\beta_2$  Cl. 1 cell line was generated with shRNA targeting 5'-CCTTGATGTCATTGTCAAT-3' and the Sh $\beta_1$  Cl. 3 cell line was created using shRNA targeting 5'-GTGATGCTGCTCACCATCA-3' in DAOY cells. Cells were passaged with 1  $\mu$ g/ml puromycin to select for knockdown cells.

### **3.3 Antibodies**

Antibodies used for western blot and immunofluorescence include: rabbit anti-Merlin (#6995), mouse anti- $\alpha$ -tubulin (#3873), anti-EGFR (#4267), rabbit anti-phospho-EGFR (Tyr1068) (#2234), rabbit anti-phospho-FAK (Tyr397) (#8556), rabbit anti-FAK (#3285), rabbit anti-phospho-YAP (Ser127) (#13008), rabbit anti-YAP (#14074) from Cell Signaling Technology (Danvers, MA); mouse anti-NF2 (sc-55575) from Santa Cruz Biotechnology (Santa Cruz, CA); rabbit anti-ATP1B1 (HPA012911) from Sigma (St. Louis, MO); rabbit anti-ATP1B2 (ab185210), mouse anti-vinculin (ab18058) and rabbit anti-paxillin (ab32084) from Abcam (Cambridge, MA). Anti-mouse and anti-rabbit (#7076S, 7074) HRP-conjugated antibodies were obtained from Cell Signaling Technology. Goat anti-rabbit Alexa-488 (A11008), goat anti-mouse Alexa-488 (A11001), donkey anti-rabbit Alexa-546 (A10040), donkey anti-mouse Alexa-546 (A10036) from Invitrogen (Waltham, MA) were used for immunofluorescence.

### **3.4 Immunoblot**

Cerebellar tissues were lysed with tissue lysis buffer (20 mM Tris-HCl, 150 mM NaCl, 1 mM EDTA, 1 mM EGTA, 1 mM  $\beta$ -glycerol phosphate, 1 mM sodium vanadate, 2.5 mM sodium pyrophosphate, 50 mM sodium fluoride, 1.2 M sodium deoxycholate, 1% IGEPAL, 1% Triton X-100, 200  $\mu$ M phenylmethylsulfonyl fluoride (PMSF)) supplemented with protease and phosphatase inhibitor cocktail, sonicated, and centrifuged at 10000 RPM for 10 min at 4°C. Cells were scraped in cold 1X PBS, centrifuged at 1000 RPM for 5 min then lysed in cold Triton X-100 lysis buffer (20 mM Tris-HCl pH 7.4, 150 mM NaCl, 1 mM EDTA, 1 mM sodium orthovanadate, 0.1% Triton X-100) supplemented with protease and phosphatase inhibitor cocktail.

Samples were reduced with 1X SDS sample buffer (0.01% SDS, 2% glycerol, 0.125 M Tris-HCl, 0.715  $\mu$ M  $\beta$ -mercaptoethanol) for 10 min at 80°C and 30 – 40  $\mu$ g of total protein was loaded into a 10% Tris-glycine polyacrylamide gel for separation.

Proteins were transferred to 0.2  $\mu$ M nitrocellulose at 100 V for 70 min. Membranes were blocked with 5% milk in Tris-buffered saline/0.1% Tween-20 (TBST) for at least 1 h before incubation in 1:1000 dilution (1:5000 for  $\alpha$ -tubulin and paxillin, 1:2000 for vinculin, 1:500 for phospho-EGFR) of primary antibody in 5% milk or 5% bovine serum albumin (BSA) in TBST for 1 h at room temperature or overnight at 4°C. After 1 h incubation in anti-rabbit or anti-mouse HRP-conjugated secondary (1:2000 – 1:5000) diluted in TBST, membranes were developed for 5 min with LI-COR reagents (LICOR, Lincoln, NE) and imaged.

For blotting proteins of similar molecular weight, membranes were incubated in stripping buffer (100  $\mu$ M  $\beta$ -mercaptoethanol, 0.06 M Tris-HCl pH 6.8, 2% SDS) at 55° for at least 30 min with occasional agitation, then washed with PBST (0.1% Tween-20 in 1X PBS) and TBST, consecutively. Membranes were probed with secondary, treated, and imaged, as described, to ensure removal of primary antibody before washing with TBST and blocking to blot for the next protein.

### **3.5 Coimmunoprecipitation**

Wild-type cerebella were collected at P6 and homogenized. After lysis with tissue lysis buffer according to the protocol described above, total protein was quantified with DC assay (Bio-Rad) and 500  $\mu$ g – 1 mg of total protein was incubated with 2  $\mu$ l anti-Merlin primary antibody or 1 mg/ml rabbit IgG overnight, then 20  $\mu$ l Protein A/G Plus-Agarose beads (Santa Cruz Biotechnology) were added and incubated for at least 2 h at 4°C. Beads were washed per product instructions (sc-2003,

Santa Cruz Biotechnology, Santa Cruz, CA), followed by sample preparation and gel electrophoresis as stated above, and western blotting was performed using the CleanBlot IP kit (Thermofisher).

### **3.6 Immunofluorescence**

To observe the cellular spatial distribution of merlin in cell lines, cells were seeded on glass coverslips, then after 16 – 24 h, serum-starved for at least 6 h and treated with a final concentration of 10 ng/ml EGF for 15 minutes. Coverslips were fixed with 4% paraformaldehyde in 1X PBS supplemented with 100  $\mu$ M  $\text{CaCl}_2$  and 1 mM  $\text{MgCl}_2$ , then quenched with 50 mM  $\text{NH}_4\text{Cl}$  for 10 – 15 min, permeabilized in 0.2% Triton X-100 in 5% BSA, and blocked in 0.1% Tween-20 in 5% BSA before staining. Permeabilized cells were stained with a 1:100 dilution of anti-Merlin overnight at 4°C. A 1:200 dilution of primary antibody was used for vinculin and phospho-YAP, 1:100 for paxillin and phospho-FAK, and 1:50 for EGFR staining. Cells were incubated in a 1:500 dilution of Alexa-488 (Merlin) and phalloidin-594 or Alexa-546 (cytoskeletal/focal adhesion proteins) secondary antibodies for 1 h at room temperature. Coverslips were mounted in Prolong Gold Antifade reagent and cured overnight at room temperature. Images were obtained with a Leica TCS SP5 confocal microscope at 63X magnification, maintaining gain and offset settings across samples stained for the same protein(s).

### **3.7 Immunohistology**

Whole brains were collected from P4 AMOG<sup>-/-</sup> litters. Age-matched AMOG<sup>-/-</sup> and WT brains were fixed in 10% neutral-buffered formalin and submitted to the Nemours Histochemistry and Tissue Processing Core Lab for sectioning and paraffin

processing. Paraffin-embedded sections were rehydrated according to standard procedure, blocked in 10% goat serum for 1 h before an overnight incubation in 1:50 primary antibody diluted in 5% goat serum/0.2% Triton X-100. Tissue samples were then stained with a 1:500 dilution of secondary antibody for 1 h. Stained tissue sections were mounted in Prolong Gold Antifade Reagent and cured overnight for confocal microscopy.

### **3.8 Merlin Double Knockdown**

DAOY vector control (ShV Cl. 1) and  $\beta_2$  knockdown (Sh $\beta_2$  Cl. 1) cells were seeded in 6-well plates, one inlaid with coverslips. Cells were transfected with 5  $\mu$ M SMARTpool NF2 siRNA or a siRNA control and DharmaFECT 1 transfection reagent (Dharmacon, Horizon Discovery Group Company, Lafayette, CO) then serum-starved overnight. After 48 h, Cells were treated with EGF for 15 min, harvested and lysed for total protein extraction. Coverslips were fixed and stained for F-actin according to the methods described above.

## Chapter 4

### RESULTS

#### 4.1 Postnatal Expression of Merlin and Associated Proteins

To analyze changes in focal adhesion proteins known to interact with Merlin, a western blot was performed using cerebellar tissues from WT and AMOG<sup>-/-</sup> mice from ages P4 to P17. Activated FAK appeared to increase postnatally, while total FAK decreased (Fig. 3). Other studies show that Merlin regulates FAK activation via Src, so p-FAK expression should have been higher in tissues with lower Merlin expression, such as the later timepoints in WT and earlier timepoints in AMOG<sup>-/-</sup> cerebellar tissue (36,43). In WT and AMOG<sup>-/-</sup> cerebella, p-YAP expression was consistent but dropped drastically after P7 (Fig. 3). Since Merlin increased postnatally in AMOG<sup>-/-</sup> cerebella, p-YAP was expected to increase because Merlin negatively regulates YAP activation (46-48). Fractionation is necessary to better understand this result, as there may be differences between nuclear and cytoplasmic protein extracts. Although p-EGFR/EGFR immunoblotting was performed, results were inconsistent and inconclusive.

In WT pups age P4 to P17, our lab previously found that Merlin decreases in the cerebellum while  $\beta_2$  increases. Merlin increased in AMOG<sup>-/-</sup> mice after P7 (Fig. 4A). The focal adhesion proteins vinculin and paxillin are consistently expressed during postnatal development in both tissue types (Fig. 4B). These results show that neither Merlin nor  $\beta_2$  expression correlate with vinculin or paxillin in the cerebellum.

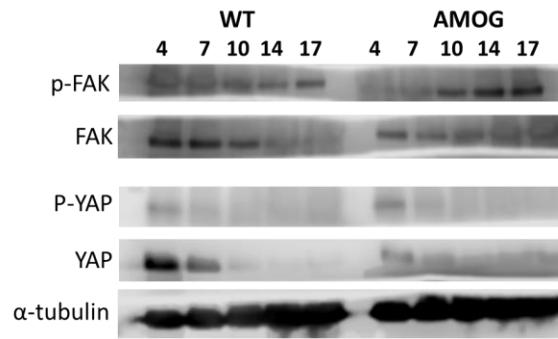


Figure 3. Postnatal expression of phosphorylated signaling proteins in WT and AMOG<sup>-/-</sup> cerebellar tissue. FAK inactivation increases in cerebellar tissue while total FAK decreases. YAP expression and inactivation was higher at earlier timepoints.

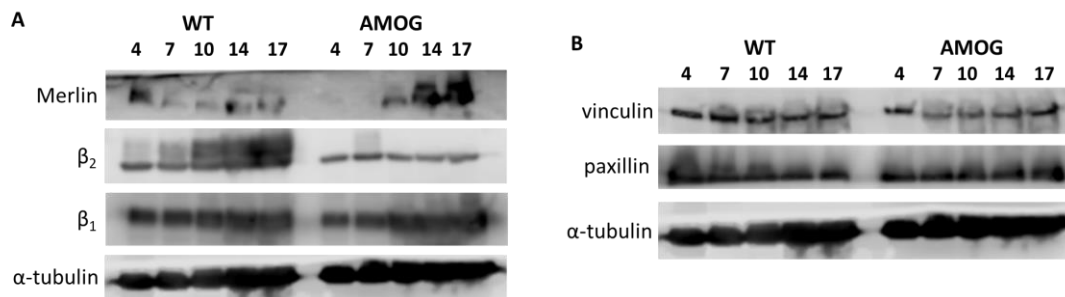


Figure 4. Postnatal β<sub>2</sub>, Merlin, and focal adhesion proteins expression in cerebellar tissue. Tissues were collected at P4, P7, P10, P14, and P17. A, Merlin increases in AMOG<sup>-/-</sup> tissue, while WT and AMOG<sup>-/-</sup> mice have B, similar levels of vinculin and paxillin.

## 4.2 Protein Localization

Merlin expression increases in β<sub>2</sub> knockdown (β<sub>2</sub> KD) cells. However, the cellular localization of Merlin in these neuronal cells is unknown. In vector control cells, actin stress fibers form, and cells elongate after EGF treatment (17). To determine Merlin's localization during these changes, β<sub>2</sub> KD cells and the

corresponding vector control were treated with EGF and stained for Merlin and actin. Double immunostaining of Merlin and p-YAP or focal adhesion proteins was also performed to observe any changes in localization in  $\beta_2$  KD cells. Unexpectedly, Merlin expression was mostly cytoplasmic. Some discontinuous membrane localization occurred in all cell lines, in both vehicle- and EGF-treated cells (Fig. 5, 6, 9, 12, 13). In previous studies, Merlin constructs localized to the plasma membrane and cytoplasm, while endogenous Merlin was mostly cytoplasmic (31,38,44,48).

#### **4.2.1 Merlin and Actin**

Merlin binds actin and has been shown to colocalize with actin in confluent cells, and our lab previously found that Merlin may be involved in the  $\beta_2$  KD related actin changes in medulloblastoma cells (44). To see if actin and Merlin colocalize in  $\beta_2$  KD cells, endogenous Merlin and F-actin were immunostained in ShV Cl. 1 and Sh $\beta_2$  cells. Merlin and F-actin localized to lamellipodia in EGF-treated control cells (Fig. 5). Similar to findings in subconfluent Schwann cells, Merlin localized to the cytoplasm in both control and knockdown cells, and both vehicle and EGF treatment conditions (Fig. 5, 6). Although Merlin membrane staining is not visible in EGF-treated  $\beta_2$  KD Figures 5, localization to the membrane is present in both conditions of  $\beta_2$  KD cells stained for p-FAK and p-YAP (Fig. 12, 13). In rounded  $\beta_2$  KD cells, there are no obvious differences in Merlin localization, which does not support my hypothesis that Merlin would be more prominent in  $\beta_2$  KD cells due to its higher levels of expression.

To clarify whether our lab's previous results were specific to  $\beta_2$ ,  $\beta_1$  KD cells (ShV Cl. 3, Sh $\beta_1$  Cl. 3) were also stained for actin to observe any changes in morphology. In  $\beta_1$  KD cells, F-actin stress fibers are disrupted but the cells do not

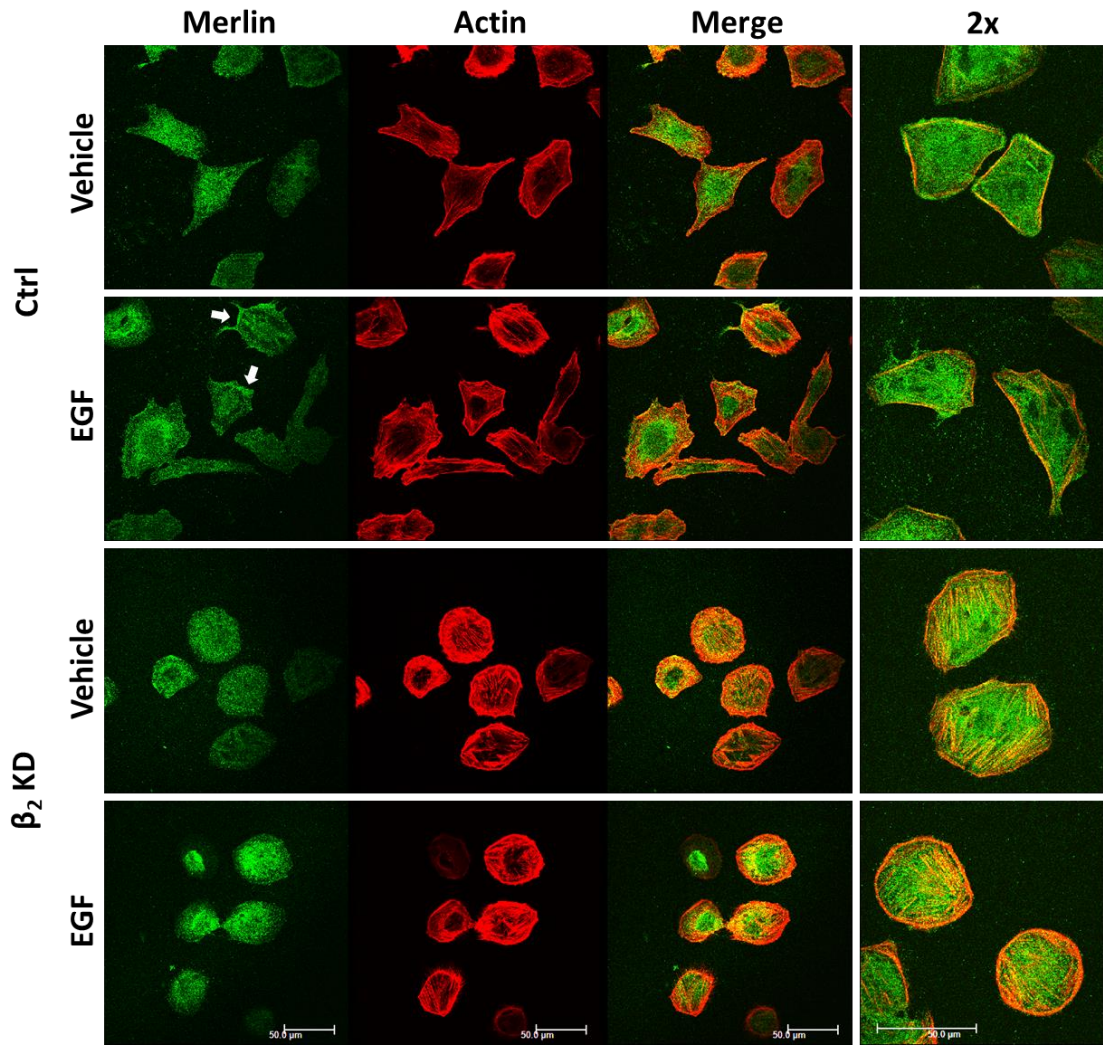


Figure 5. Merlin and actin localization in  $\beta_2$  knockdown cells. Cells were seeded at low density and treated with EGF for 15 min before fixation. Control cells elongate and form actin stress fibers when induced with EGF.  $\beta_2$  KD cells remain rounded after EGF treatment. Merlin is found in the cytosol regardless of cell type or treatment and localizes to membrane of some control cells. White arrow indicates lamellipodia localization. Scale bar: 50  $\mu\text{m}$ .

have the rounded morphology phenotype of  $\beta_2$  KD cells (Fig. 6).  $\beta_1$  KD cells elongate when induced with EGF, as seen previously in our lab with DAOY and  $\beta_2$  KD control

cells. Vehicle-treated  $\beta_1$  KD cells do not have Merlin membrane staining in Fig. 6, but some membrane staining is visible in  $\beta_1$  KD cells co-stained for vinculin (Fig. 9). Given the variability in Merlin membrane localization in both  $\beta_2$  KD and  $\beta_1$  KD cells, it is difficult to define the effects of EGF treatment on Merlin localization.

#### **4.2.2 Merlin and EGFR**

EGFR signaling is prolonged in  $\beta_2$  knockdown cells (17). To determine if Merlin and EGFR localization overlap since Merlin is known to regulate EGFR mobility,  $\beta_2$  knockdown cells were stained for both proteins (44). In EGF-treated cells, internalized EGFR was expected. Endosomal staining is visible for both EGF-treated cell types and its localization is more compact in  $\beta_2$  KD cells (Fig. 7). Vehicle-treated control cells had more EGFR localize to focal points of the membrane than vehicle-treated, rounded  $\beta_2$  KD cells. EGFR was also found in cellular extensions in EGF-treated  $\beta_2$  KD cells. Merlin was not associated with the vesicle membranes of internalized EGFR.

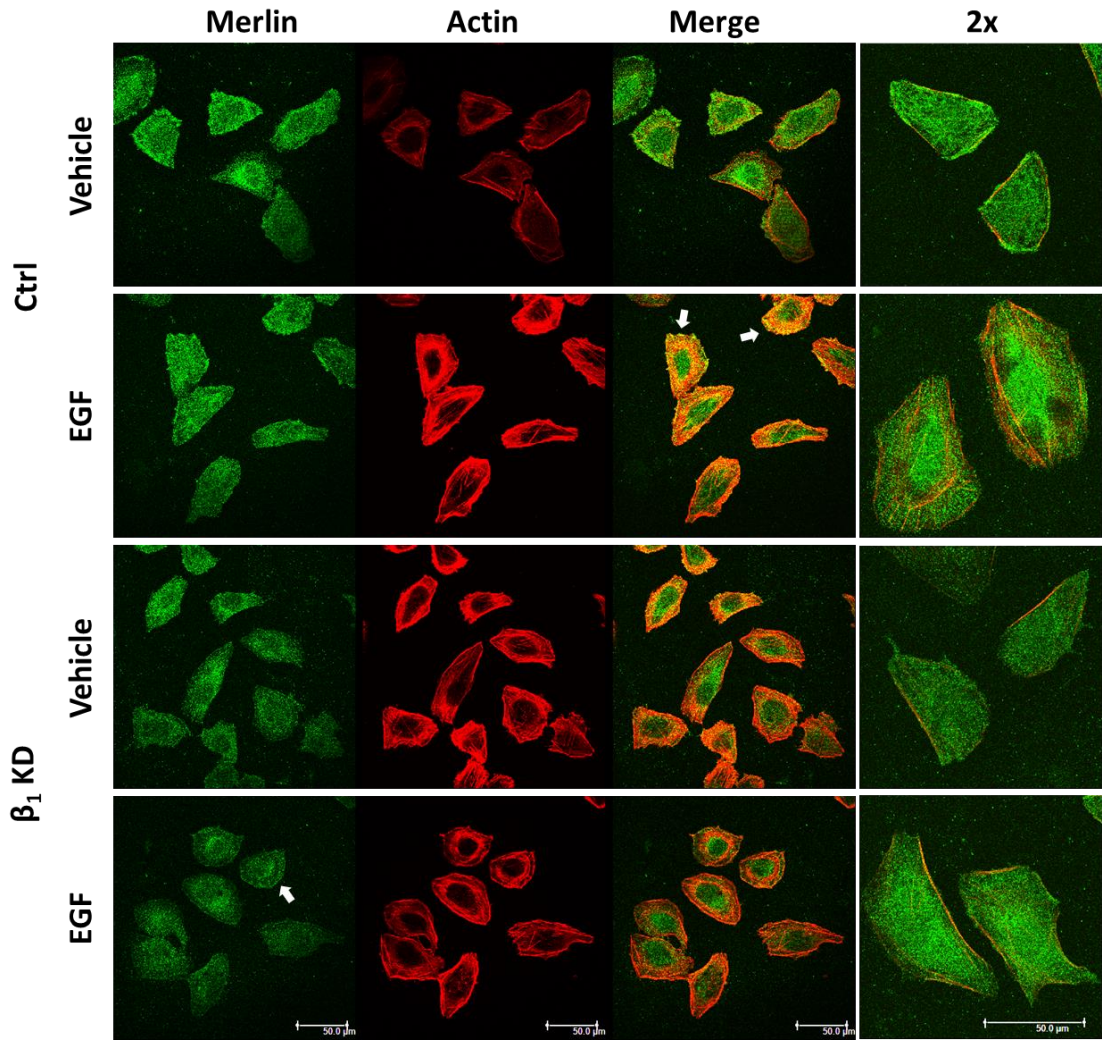


Figure 6. Merlin and actin localization in  $\beta_1$  knockdown cells. Cells were seeded at low density and treated with EGF for 15 min before fixation. Cell morphology and actin organization for  $\beta_1$  KD cells are comparable to control cells. White arrows indicate lamellipodia localization. Scale bar: 50  $\mu$ m.

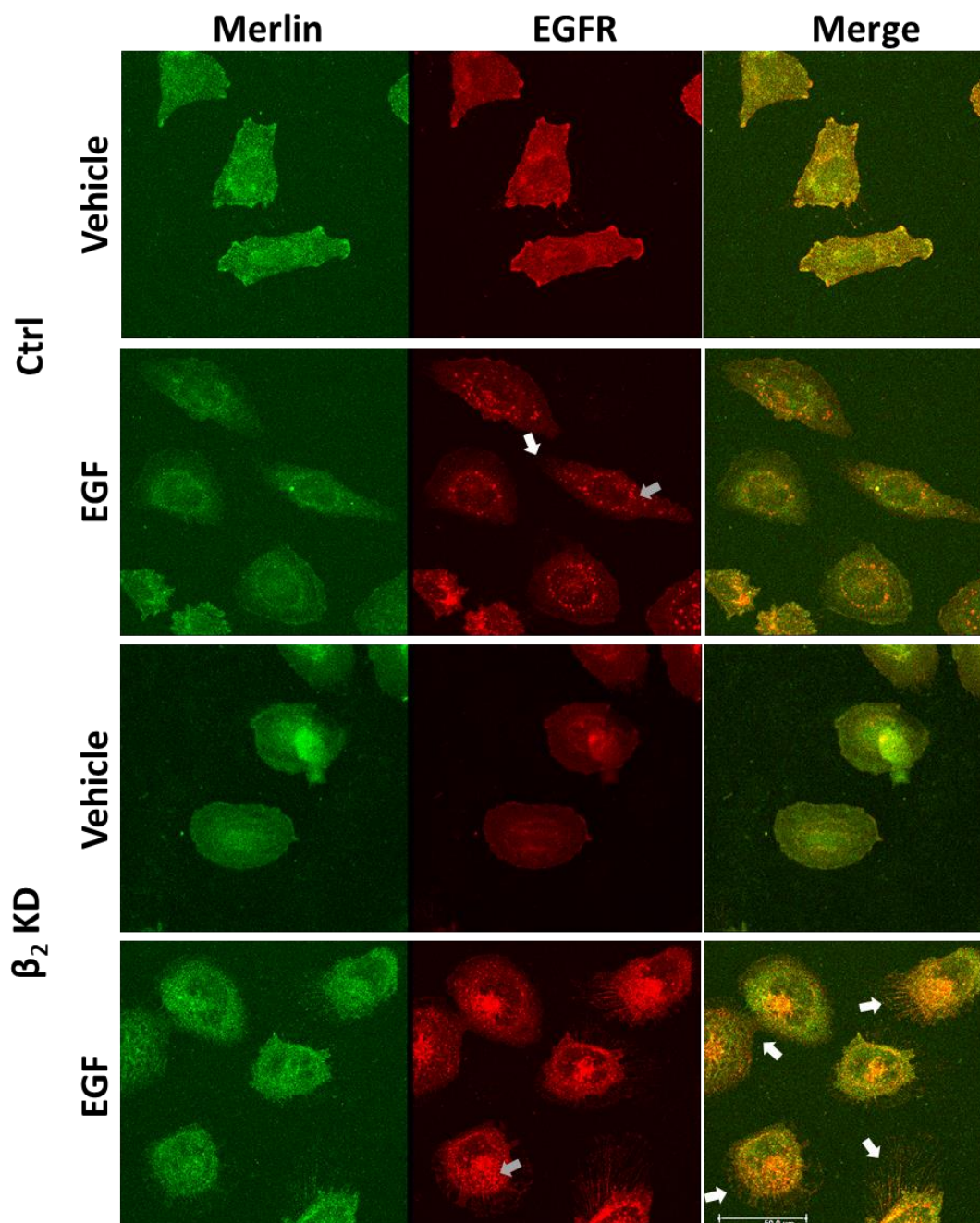


Figure 7. Merlin and EGFR localization in  $\beta_2$  knockdown cells. Cells were seeded at low density and treated with EGF for 15 min before fixation. Internalized EGFR localizes around the nucleus after EGF treatment. White arrows indicate cellular extensions, gray arrows indicate internalized EGFR. Scale bar: 50  $\mu$ m.

### 4.2.3 Merlin and Focal Adhesion Proteins

Previous studies have shown that paxillin and FAK colocalize, and that vinculin localizes to focal adhesions (42,44,49). Merlin is known to regulate FAK and paxillin in glial cells (36), and vinculin in epithelial cells (44). The spatial relation of these proteins to Merlin in neurons is unknown, and whether the loss of  $\beta_2$  affects their localization is also unknown. To characterize the localization of these proteins in neurons and compare them to Merlin localization in  $\beta_2$  KD cells, double immunostaining was performed on vehicle- and EGF-treated cells. In all cell types, vinculin expression was found at the cell membrane, at focal adhesion sites and the cytoplasm, in both treatment conditions. This is congruent with previous findings in confluent epithelial cells (44,49). Some cells in each treatment condition had focal adhesion sites containing both Merlin and vinculin for  $\beta_2$  KD vector control cells,  $\beta_2$  KD cells, and  $\beta_1$  KD cells. In  $\beta_2$  KD control cells, EGF-treated  $\beta_1$  KD and  $\beta_2$  KD cells, strong staining of perinuclear vinculin was also visible (Fig. 8, 9).

Paxillin and Merlin had similar cytoplasmic expression in most of the cell lines and across both treatment conditions, although staining in  $\beta_1$  KD control cells was faint. Paxillin was present in focal adhesions at the basal level and its localization did not change in EGF-treated cells (Fig. 10, 11). Paxillin localization to the cytoplasm was not as obvious in EGF-treated  $\beta_2$  KD cells, when compared to the control cells, but was visible in the magnified images (Fig. 10). Phospho-FAK and Merlin expression overlapped at some sites of adhesion and at the cell membrane in EGF-treated control and  $\beta_2$  KD cells (Fig. 12). These findings align with the current understanding of Merlin's interaction with paxillin and its association with focal adhesions. Based on Merlin's higher expression in  $\beta_2$  KD cells, I had hypothesized that Merlin, and subsequently, downstream or associated focal adhesion proteins like

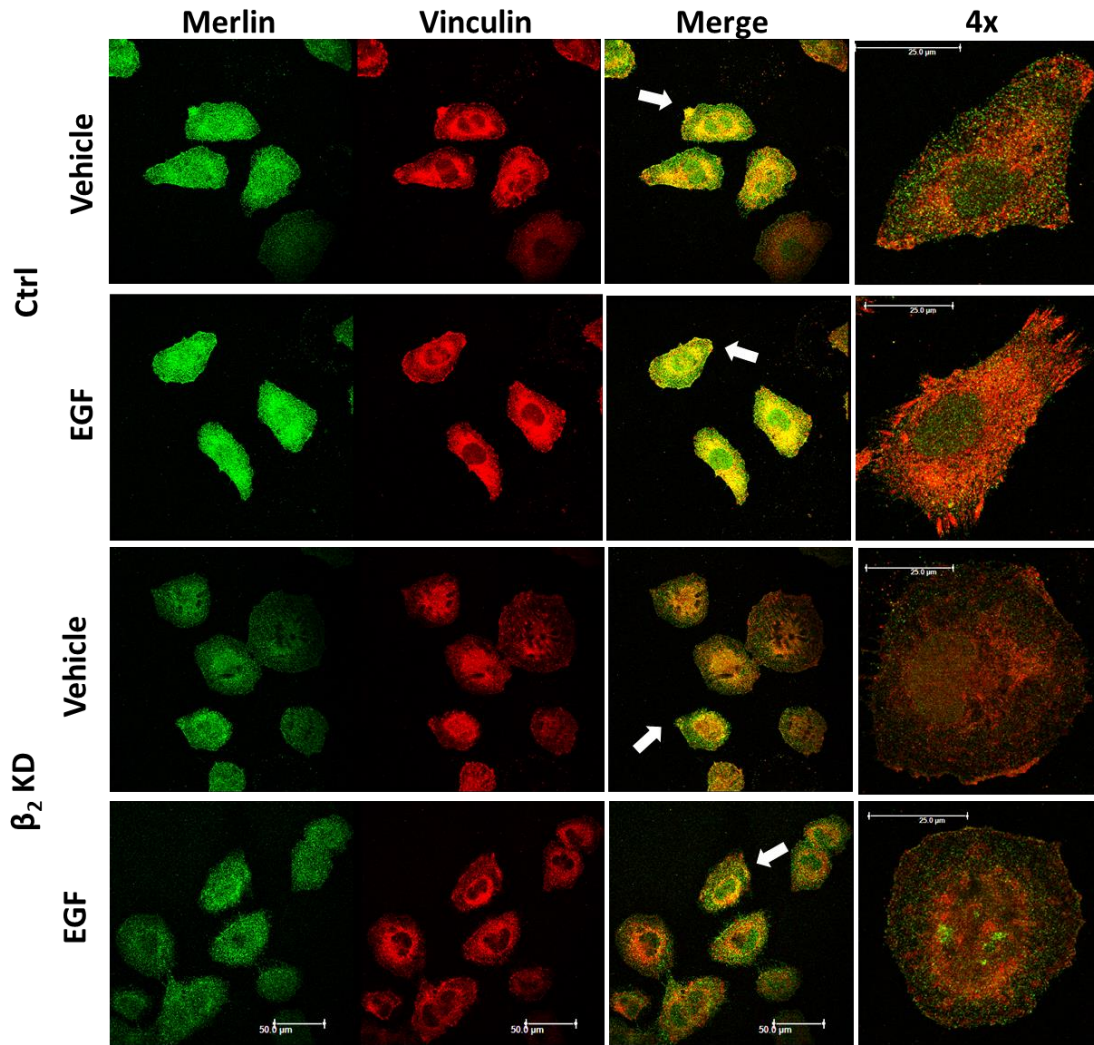


Figure 8. Merlin and vinculin localization in  $\beta_2$  knockdown cells. Cells were seeded at low density and treated with EGF for 15 min before fixation. Merlin and vinculin localize to focal adhesions. White arrows indicate areas of overlapping Merlin and vinculin localization. Scale bar: 50  $\mu$ m, 25  $\mu$ m for 4x.

FAK and paxillin would be more prominent in  $\beta_2$  KD cells. This hypothesis was not supported, as a noticeable difference in Merlin immunofluorescence was not seen in  $\beta_2$

KD cells. Quantitative microscopy would need to be performed to obtain a more definitive result.

#### **4.2.4 Merlin and Phospho-YAP**

In epithelial cells, YAP localized to the cytoplasm and the nucleus depending on cell density (48). To visualize the state of inactivated YAP in  $\beta_2$  knockdown cells, fixed cells were stained for p-YAP and Merlin. Although p-YAP was expected to be largely cytoplasmic, p-YAP also localized to the cell membrane in  $\beta_2$  KD cells (Fig. 13). YAP interacts with Merlin's C-terminus, and Merlin is also a scaffold for the kinases that phosphorylate YAP (39,47). This scaffold function of Merlin could be responsible for the faint membrane staining of YAP seen in  $\beta_2$  KD cells, but more experiments would be necessary. These images were obtained from low density cell cultures, so additional experiments would need to be conducted in higher density cell cultures to see if this result is replicated. It is interesting, however, that Merlin also localizes to the same areas of the cell membrane as YAP in  $\beta_2$  KD cells and vehicle-treated control cells.

#### **4.2.5 Summary of Localization Results**

EGF treatment did not have a visible effect on the localization of focal adhesion proteins in  $\beta_2$  KD cells. There were also no visible changes in Merlin localization in EGF-treated cells, according to these qualitative results. These findings do not support my hypothesis that Merlin and associated proteins (i.e, paxillin) would be more detectable in EGF treated and  $\beta_2$  KD cells, nor my hypothesis that actin and Merlin would colocalize to a greater extent in  $\beta_2$  KD cells. Merlin was not seen in endosomes containing EGFR in EGF-treated cells, but internalized EGFR localization

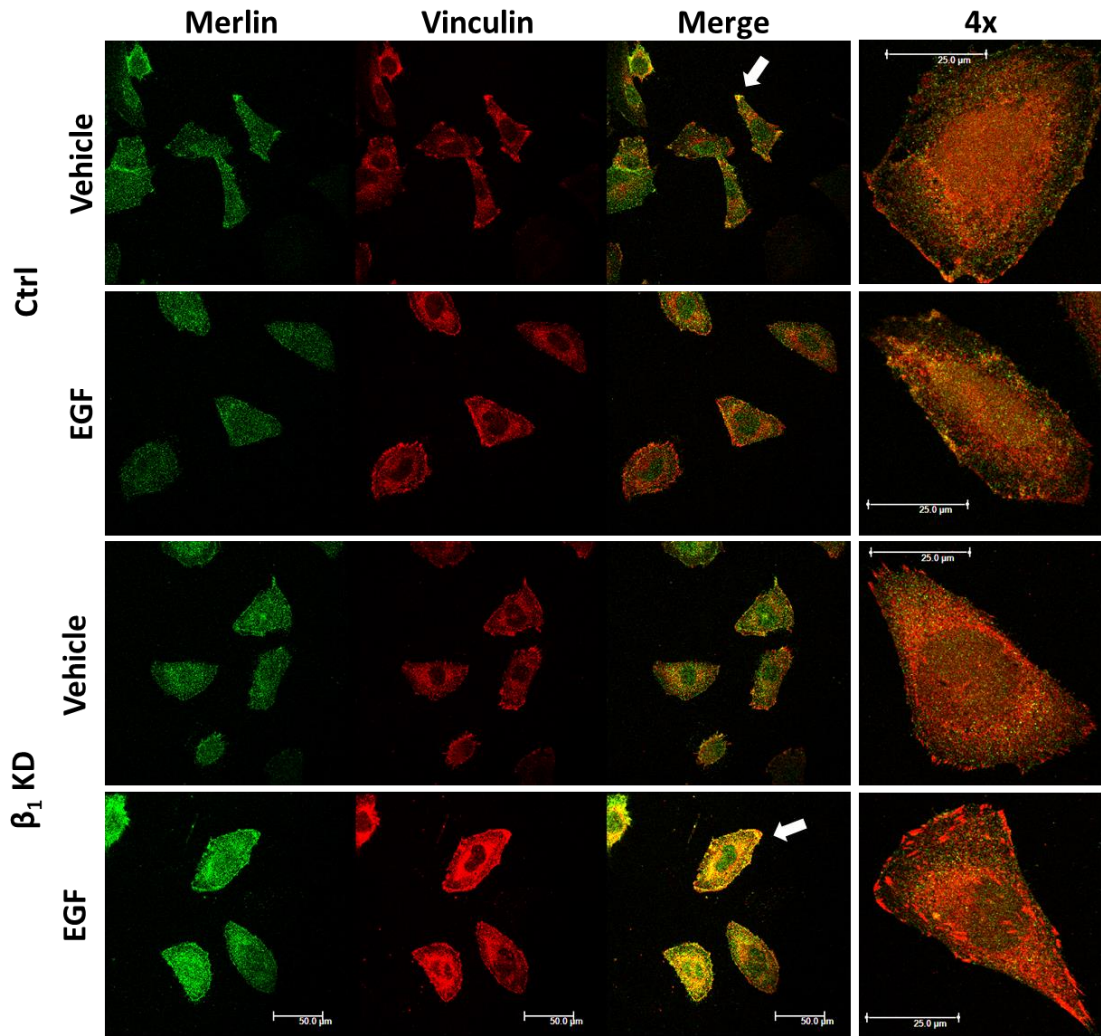


Figure 9. Merlin and vinculin in  $\beta_1$  knockdown cells. Cells were seeded at low density and treated with EGF for 15 min before fixation. Immunofluorescence experiments were repeated in  $\beta_1$  KD cells to determine if colocalization was specific to  $\beta_2$  deficiency. Both basal and cytoplasmic vinculin staining is present in  $\beta_1$  KD cells. White arrows indicate localization of vinculin and Merlin to focal adhesion. Scale bar: 50  $\mu$ m.

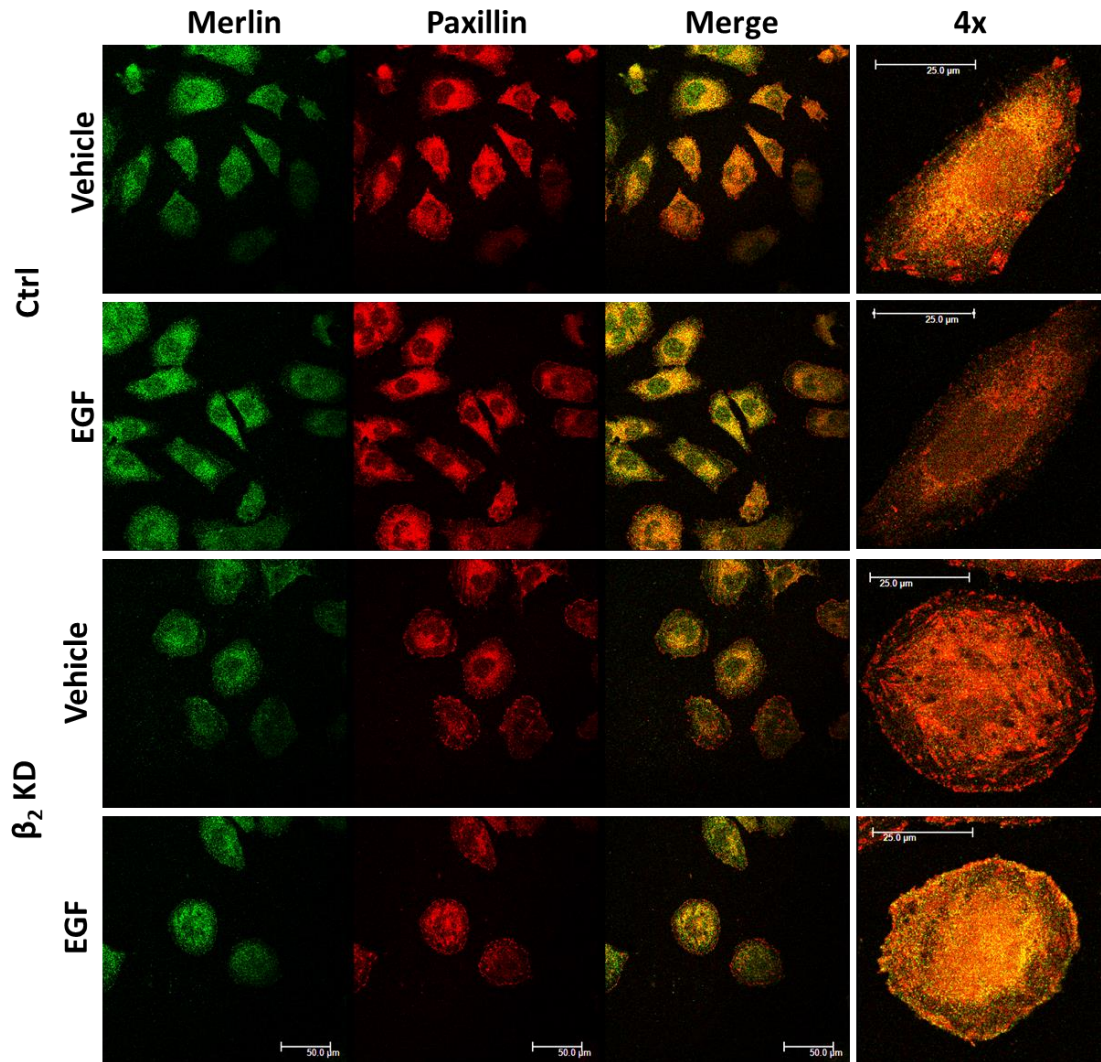


Figure 10. Merlin and paxillin localization in  $\beta_2$  knockdown cells. Cells were seeded at low density and treated with EGF for 15 min before fixation. Punctate paxillin staining was observed in the basolateral membrane, in addition to cytoplasmic expression. White arrows indicate Merlin and paxillin localization at the centrosome. Scale bar: 50  $\mu\text{m}$ , 25  $\mu\text{m}$  in 4x.

did differ between control and  $\beta_2$  KD cells. YAP inactivation and localization to the cytoplasm was not more evident in  $\beta_2$  KD cells, but an unexpected localization to the membrane was observed. Coimmunoprecipitation is needed to confirm possible

relation to paxillin, phospho-FAK, and vinculin seen in the occasional localization of Merlin to focal adhesion sites where these proteins are expressed.

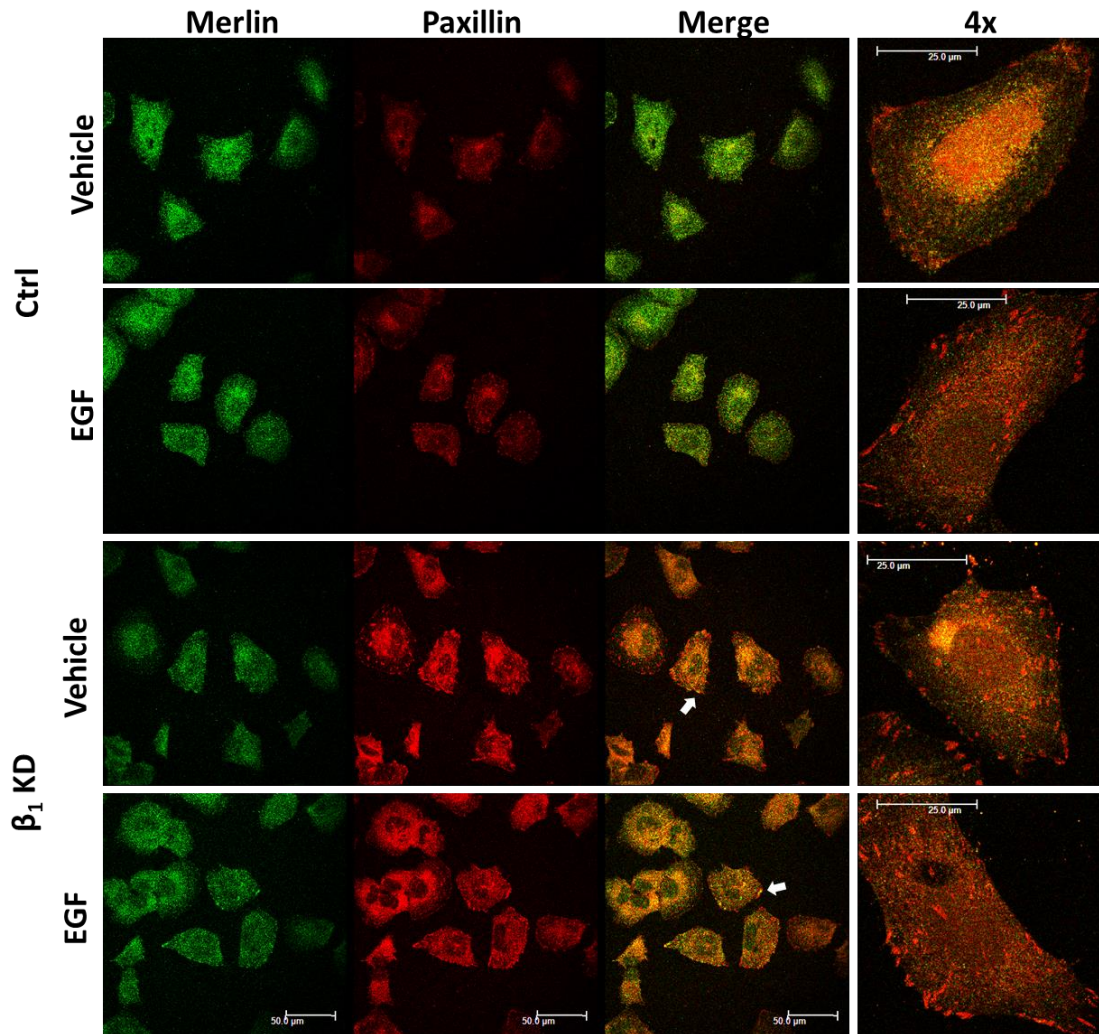


Figure 11. Merlin and paxillin in  $\beta_1$  knockdown cells. Cells were seeded at low density and treated with EGF for 15 min before fixation. Paxillin localizes to focal adhesions and the cytoplasm in both control and  $\beta_1$  KD cells. White arrows indicate localization of both Merlin and paxillin at focal adhesions. Scale bar: 50  $\mu\text{m}$ .

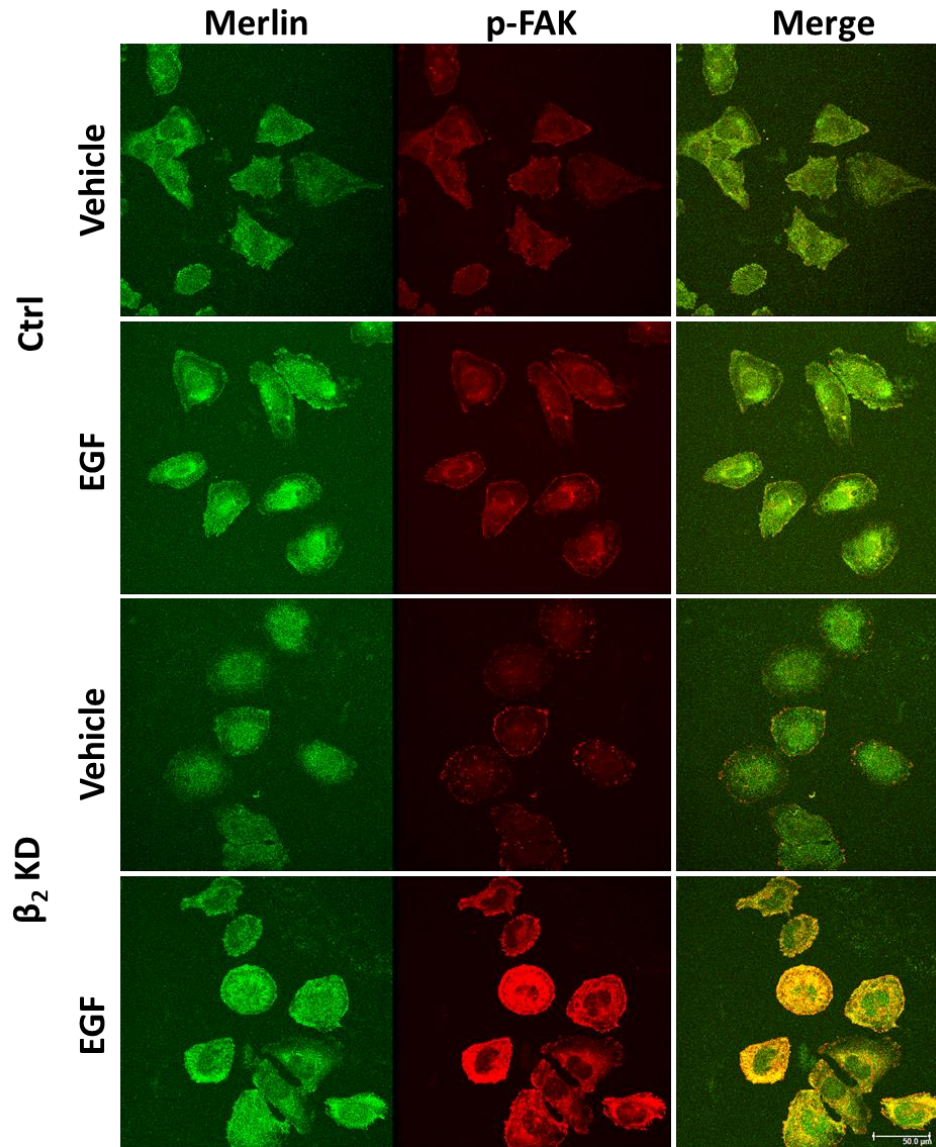


Figure 12. Merlin and phospho-FAK localization in  $\beta_2$  knockdown cells. Cells were seeded at low density and treated with EGF for 15 min before fixation. Phospho-FAK and Merlin localize to the membrane of some EGF-treated cells of both cell lines, with higher expression in  $\beta_2$  KD cells. In vehicle-treated  $\beta_2$  KD cells, punctate staining similar to paxillin is visible. Scale bar: 50  $\mu$ m.

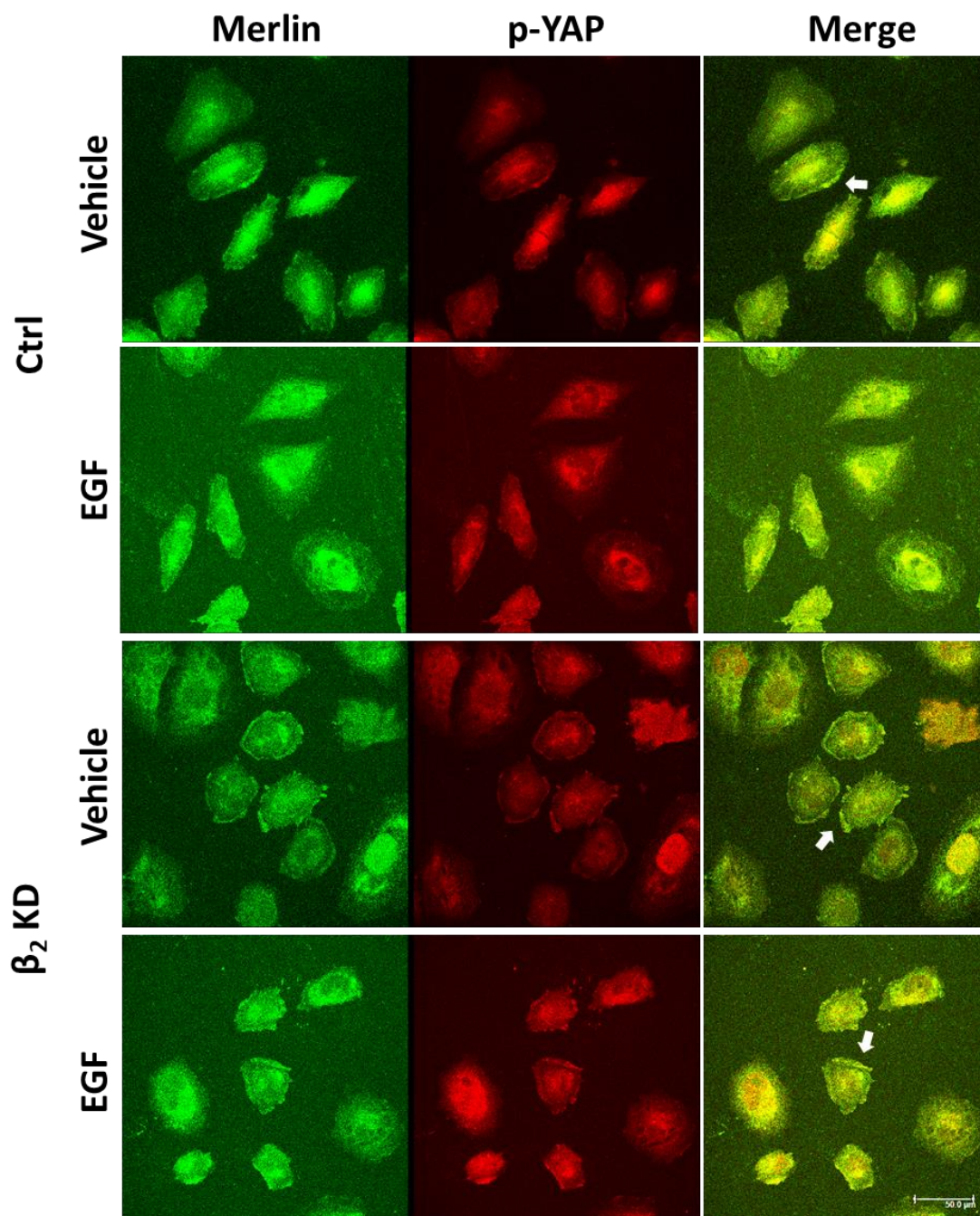


Figure 13. Merlin and phospho-YAP localization in  $\beta_2$  knockdown cells. Cells were seeded at low density and treated with EGF for 15 min before fixation. Phospho-YAP localizes to the cytoplasm and the cell membrane in  $\beta_2$  KD cells and can be also seen at some focal adhesions in  $\beta_2$  KD and control vehicle-treated cells. Scale bar: 50  $\mu$ m.

### 4.3 Coimmunoprecipitation

To confirm which proteins are associated with Merlin and focal adhesion complexes, a Merlin antibody was used to pull down proteins in WT cerebellar tissue. Neither EGFR nor vinculin were pulled down in complex with Merlin in WT tissue (Fig. 14). These results are inconclusive due to the inconsistency between replicates. In fibroblasts and epithelial cells, Merlin precipitates with EGFR, so it was expected that EGFR would be detected but that result could not be replicated here (33). Inconclusive results were obtained when blotting for paxillin and when the assay was performed using AMOG<sup>-/-</sup> tissue and DAOY knockdown cells. Further optimization is needed to see whether Merlin binds, directly or indirectly, to EGFR, paxillin, and vinculin.

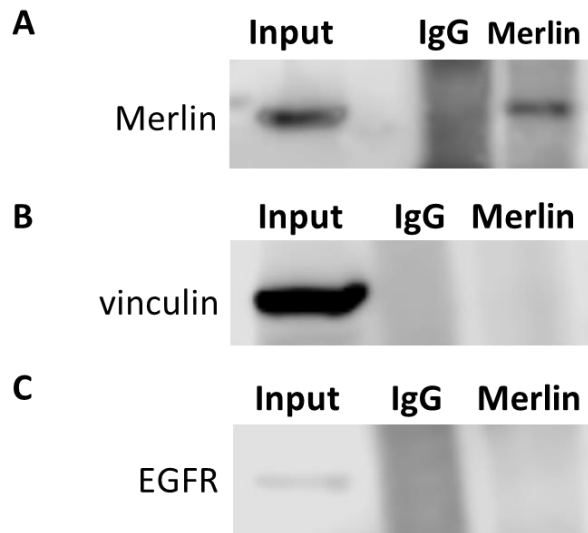


Figure 14. Coimmunoprecipitation targeting Merlin-associated proteins in WT cerebellum. Pups were sacrificed at P6 and cerebellar tissues were lysed, total protein extracted, then diluted and incubated with 1  $\mu$ g rabbit IgG or 1  $\mu$ l anti-NF2 to pull down Merlin-associated protein complexes. A, Confirmation of Merlin protein in pull-down product. B, Vinculin and C, EGFR did not precipitate with Merlin.

#### 4.4 Merlin Knockdown

Merlin knockdown was performed in  $\beta_2$  KD cells to determine whether the round morphology of  $\beta_2$  KD cells that is maintained after EGF treatment would be reversed. Although there are some effects (apoptotic cells) of the transient transfection with siRNA (Fig. 15A), the cortical actin ring was reversed in  $\beta_2$  KD/NF2 KD cells, as elongation of cells and formation of longer stress fibers were observed (Fig. 15B). This result confirms Merlin's involvement in changes in actin organization and morphology in  $\beta_2$  KD cells.

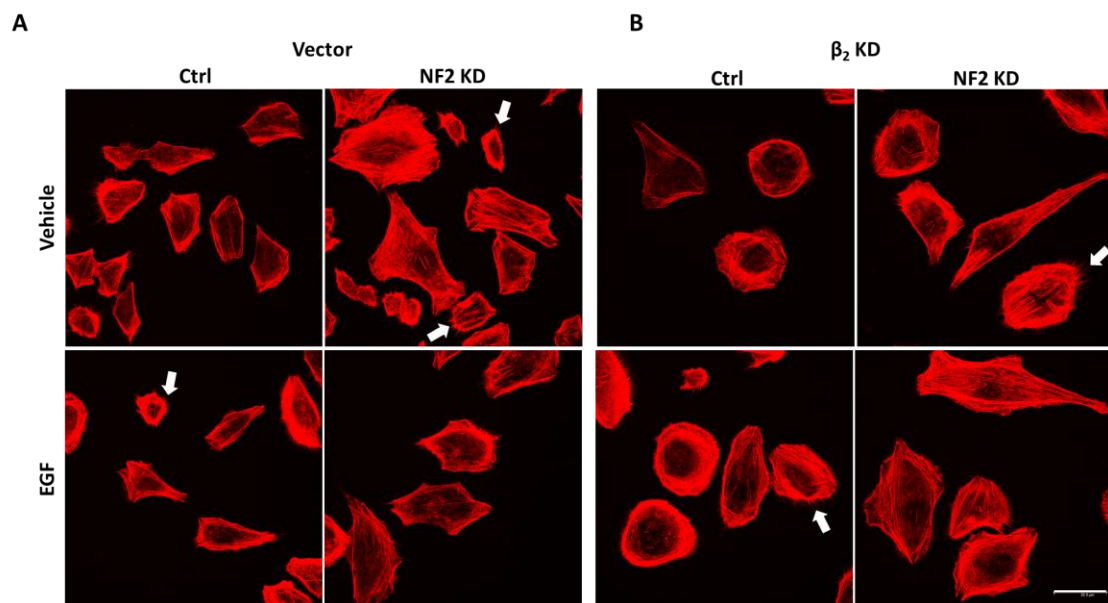


Figure 15. Merlin knockdown in  $\beta_2$  knockdown cells. Cells were transfected with NF2 siRNA or siCtrl and seeded at low density, before treatment with 10 ng/ml EGF for 15 min and fixation.  $\beta_2$  KD cells' rounded phenotype reversed by NF2 KD, and cell elongation is observed in EGF treated cells. White arrows indicate actin extensions. Scale bar: 50  $\mu$ m.

## 4.5 Immunohistochemistry

Cerebellar granule cell progenitors reach the peak of proliferation at P6, after which they migrate to form the inner granule layer. Here we see that Merlin expression was higher in and localized to the periphery of granule cells (Fig. 16). There was also Merlin expression in the cytoplasm of the neighboring Purkinje cells, with particularly strong staining at P4 for both WT and AMOG<sup>-/-</sup> tissue. Merlin and actin expression were similarly distributed, as expected. These data also show higher Merlin expression at later timepoints in AMOG<sup>-/-</sup> cerebellum, but replicates are needed to confirm this result. Although there seems to be differences in tissue morphology in AMOG<sup>-/-</sup> cerebellum at P4, H&E staining confirmed that this irregularity in the Purkinje cell layer was not unique to the AMOG<sup>-/-</sup> cerebellum (see Appendix B).

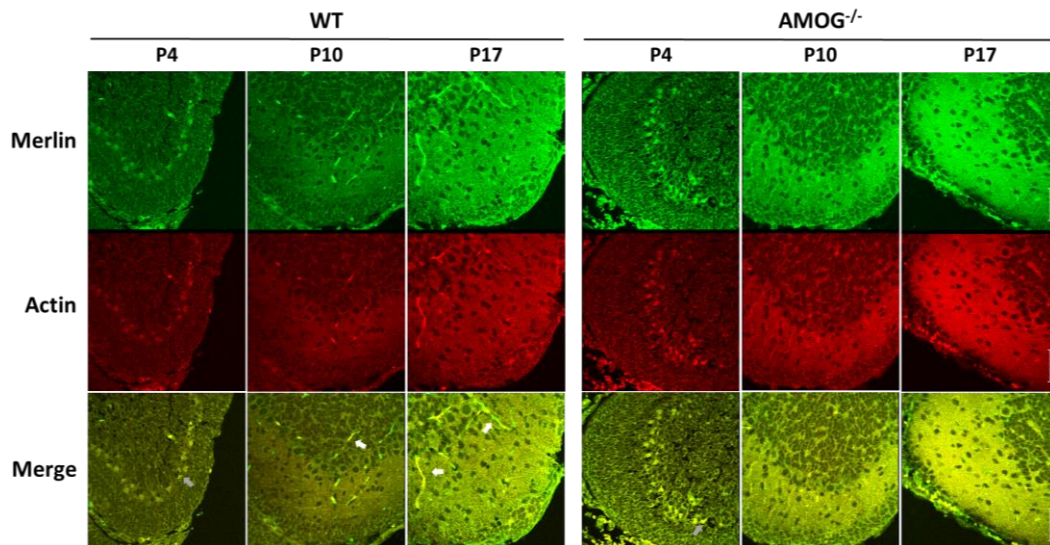


Figure 16. Merlin and actin in postnatal WT and AMOG<sup>-/-</sup> cerebellar tissue. The inner granule cell layer has not formed completely in P4 mice. Actin and Merlin expression was high in the periphery of CGP cells and the cytoplasm of Purkinje cells (gray arrows) in AMOG<sup>-/-</sup> mice. Merlin and actin were expressed in WT differentiating neurons at P10 and P17. Scale bar: 50  $\mu$ m.

Merlin and EGFR localization was analyzed in the same cerebella. EGFR was expected to be expressed in both CGP cells and Purkinje cells, mostly around the edges of the cells and to some extent in the cytoplasm. Merlin and EGFR localization patterns also overlapped in WT and AMOG<sup>-/-</sup> cerebellar tissue, with localization to the periphery of cerebellar granule cells at all timepoints (Fig. 17). Both Merlin and EGFR localized to the cytoplasm of Purkinje cells at P4. Although Merlin's localization to elongated neurons is not as visible in these images, there were some neurons with strong Merlin staining, but not EGFR, at the later timepoints.

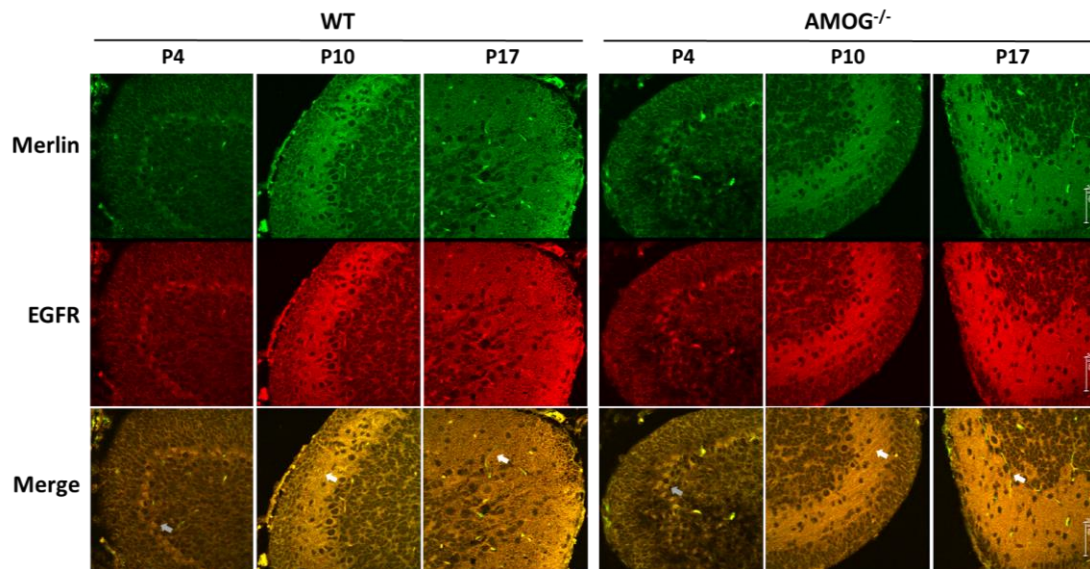


Figure 17. Merlin and EGFR in postnatal WT and AMOG<sup>-/-</sup> cerebellar tissue. Both Merlin and EGFR localize around the cerebellar granule cell progenitors. At P4, both proteins were found in the cytoplasm of Purkinje cells (gray arrows). Some staining of elongated, differentiated neurons and branched (WT) or extended projections (AMOG<sup>-/-</sup>) were visible (white arrows). Scale bar: 50  $\mu$ m.

Perinuclear EGFR was observed in both WT and AMOG<sup>-/-</sup> sections at P10. At P10 and P17, Merlin and EGFR were seen in axons and dendrites underlying the external granule layer in both WT and AMOG<sup>-/-</sup> cerebella although the patterns look different, with some branching in the WT tissue. Blots for EGFR activation in cerebellar tissue were inconclusive, so it is difficult to interpret these results on their own. However, overlap of Merlin and EGFR in both WT and AMOG<sup>-/-</sup> cerebella was confirmed.

## Chapter 5

### DISCUSSION

Na,K-ATPase  $\beta_2$  deficient cells and cerebellar tissue have shown an increase in Merlin (17). This increase in Merlin could affect the structures which Merlin regulates and supports. To determine whether Merlin is part of focal adhesions and actin organization in neuronal cells, Merlin's protein levels and localization were characterized in  $\beta_2$  deficient cerebellar tissue and medulloblastoma cells. Merlin was found at focal adhesion sites and in the cytosol of  $\beta_2$  knockdown cells. In WT and AMOG<sup>-/-</sup> cerebellar tissue, Merlin was observed in Purkinje cells and around granule cells. While Merlin is known to interact with focal adhesion proteins and junctional complexes in glial and epithelial cells, both its role in the nucleus and whether it serves the same functions in neurons is unclear.

#### 5.1 Merlin and Focal Adhesion Proteins

In AMOG<sup>-/-</sup> cerebellar tissue, Merlin increases postnatally. Vinculin, p-FAK, and paxillin levels were consistent throughout P4 to P17 in AMOG<sup>-/-</sup> mice and WT cerebella, while total FAK, p-YAP, and total YAP decreased. *In vitro* results showed discontinuous Merlin expression at the cell membrane sometimes overlapped with vinculin, paxillin, and activated FAK at some points, but Merlin localization was mostly cytosolic. The localization of focal adhesion proteins generally remained the same in all cell lines when cells were treated with EGF.  $\beta_2$  knockdown cells did not have any obvious differences in localization of the focal adhesion proteins when compared to control cells, although cytoplasmic staining of vinculin and paxillin was not as strong in some  $\beta_2$  KD cells compared to the control cells. EGF-treated  $\beta_2$  KD

cells did have strong staining of p-FAK at focal adhesions, compared to controls, but quantitative microscopy would be needed to give a more conclusive result.

According to the blots in cerebellar tissue, FAK and YAP expression may be proteins that are affected that by  $\beta_2$  KD and the resulting increase in Merlin. In  $\beta_2$  KD cells, phospho-YAP surprisingly localized to the membrane, along with Merlin. YAP expression is usually either cytoplasmic or nuclear. Higher density regions of  $\beta_2$  KD cells did contain some cells with nuclear localization. Our lab found that  $\beta_2$  deficiency results in an increase in p-YAP and p-FAK (25). The changes in p-YAP could not be addressed by the immunofluorescence results in this study, as cell cultures were not grown to confluency.

While YAP was unexpectedly found at the cell membrane, actin and Merlin did not colocalize at the membrane or near of stress fibers in  $\beta_2$  KD cells as hypothesized. F-actin and Merlin did localize to lamellipodia in some EGF-treated control cells, though. This may be due to the primary antibody specificity, as Merlin has 10 isoforms and slight differences were observed in membrane expression of Merlin between antibodies. Actin stress fiber disruption and the rounded cell morphology in  $\beta_2$  knockdown cells was reversed by Merlin knockdown. Establishing a stable NF2 KD cell line would be useful for also determining the effect of NF2 KD in control cells, as the differences seen here may be an artifact of transfection. *In vivo*, Merlin expression appeared higher in the external granule layer of AMOG<sup>-/-</sup> cerebellum at P4 and in some differentiated neurons at later timepoints. However, more replicates are necessary to confirm these findings.

EGF was used to induce actin stress fibers for these experiments and, as a result, EGFR was internalized in EGF-treated control and  $\beta_2$  KD cells. Membrane

bound EGFR was present in some of the same regions as Merlin in vehicle-treated control cells. In EGF-treated cells, EGFR localization differed between cell lines, with  $\beta_2$  KD cells lacking the more distributed localization of endosomal EGFR seen in control cells. Whether this is related to the difference in actin organization and cell morphology remains to be determined. There were also cellular extensions where weak staining of Merlin and EGFR is visible in EGF-treated  $\beta_2$  KD cells. In cerebellar tissue, both Merlin and EGFR were present in neuron projections at P10. Blots for p-EGFR/EGFR and coimmunoprecipitation of EGFR in cerebellar tissue were inconclusive, so the activation state of EGFR will need to be ascertained in future studies.

The results described here support Merlin's established association with paxillin, vinculin, and p-FAK in cells of neuronal lineage. EGF treatment does not appear to affect the localization of these proteins, but the localization of internalized EGFR is affected by  $\beta_2$  knockdown. Phospho-YAP was found to localize to the membrane in  $\beta_2$  KD cells and, out of the set of proteins studied, total YAP is diminished in AMOG<sup>-/-</sup> cerebellar tissue while Merlin increases. Merlin localization to Purkinje cells and cerebellar granule cells was also confirmed in cerebellum, along with EGFR and actin. To further characterize Merlin's functions in the developing cerebellum, future studies in these or similar models should investigate the EGFR and Hippo-YAP signaling pathways.

## **5.2 Future Directions and Considerations**

To clarify the results of p-FAK and p-YAP localization in  $\beta_2$  knockdown cells, total FAK and total YAP localization should be assessed.  $\beta_1$  knockdown cells should also be analyzed to determine if the results for EGFR, p-FAK, and p-YAP are specific

to  $\beta_2$ . Coimmunoprecipitation experiments yielded inconclusive results for paxillin, EGFR, and vinculin interactions with Merlin. The protocol needs to be optimized for AMOG<sup>-/-</sup> cerebellum and  $\beta_2$  KD cells to provide supporting evidence for the immunofluorescence results.

A major factor in Merlin expression and function is cell density. The results obtained in this study were based on experiments using low density cells, while Litan et al. used confluent, trypsinized cells for immunoblots. Future work needs to differentiate between cell density-dependent effects and  $\beta_2$ -dependent effects in  $\beta_2$  knockdown cells, and also to evaluate whether trypsin affects the expression of focal adhesion proteins. It would be beneficial to also test primary cultures or other neuronal cells, since the localization results are against the background of medulloblastoma cells. Primary cultures of WT CGP cells required high cell density and a laminin and poly-D-lysine coated surface for differentiation (see Appendix C). Providing some substrate for cells to attach to may change the outcomes found in this study, especially since  $\beta_2$  and Merlin are directly related to cell-cell contact and cell-matrix interactions.

In terms of molecular studies, there are many directions in which future work can proceed. Merlin knockdown rescued the actin disorganization phenotype of  $\beta_2$  KD cells, so more experiments are needed to find whether vinculin and paxillin localization changes in Merlin/ $\beta_2$  double knockdown cells. In neurobasal medium,  $\beta_2$  knockdown cells fail to form medullospheres and cells adhere to the dish surface (Fig. D1). This supports  $\beta_2$  involvement in cell-cell adhesion, but more evidence is needed to clarify whether this is a  $\beta_2$  isoform specific result.  $\beta_2$  knockdown cell phenotypes were rescued by  $\beta_2$ -YFP, so to determine whether the adhesion function is responsible for these phenotypes, a  $\beta_2$  construct with mutated glycosylation sites could be used.

Another option would be to knockdown  $\alpha_2$ , since  $\beta_2$  reduces pump activity and the changes observed so far may be caused by a defunct Na,K-ATPase.

Na,K-ATPase  $\beta_2$  deficiency was shown to correlate with a decrease in YAP and slight differences in p-FAK, vinculin, and p-YAP overlap with Merlin distribution compared to controls. The implications of an increase in Merlin association with focal adhesion proteins and internalized EGFR are not fully understood. Merlin research has focused on Merlin deficiency and the resulting tumors and neuropathy that occurs. Little is known about Merlin overexpression, and even less is known about Na,K-ATPase  $\beta_1$  and  $\beta_2$  and their relevance, if any, in disease. The characterization of Merlin localization in this study was conducted in DAOY cells, which provided a stem cell and tumorigenic background. Future work should clarify whether these findings are of any relevance to oncogenesis and metastasis, both of which are affected by cell-cell and cell-ECM interactions.

## REFERENCES

1. Mobasheri, A. a. A. J. a. C.-C. I. a. B. M. D. a. T. M. a. F. M. J. O. a. L. J. F. a. M.-V. P. (2000) Na<sup>+</sup>, K<sup>+</sup>-ATPase isozyme diversity; Comparative biochemistry and physiological implications of novel functional interactions. *Bioscience Reports* **20**, 51-91
2. Kaplan, J. H. (1985) Ion Movements Through the Sodium Pump. **47**, 535-544
3. Larsen, B. R. a. S. A. a. M. N. (2016) Managing Brain Extracellular K<sup>(+)</sup> during Neuronal Activity: The Physiological Role of the Na<sup>(+)</sup>/K<sup>(+)</sup>-ATPase Subunit Isoforms. *Frontiers in Physiology* **7**, 141
4. Rajasekaran, S. A., Palmer, L. G., Quan, K., Harper, J. F., Ball, W. J., Bander, N. H., Soler, A. P., and Rajasekaran, A. K. (2001) Na,K-ATPase  $\alpha$ -Subunit Is Required for Epithelial Polarization, Suppression of Invasion, and Cell Motility. **12**, 279-295
5. Rajasekaran, S. A., Palmer, L. G., Moon, S. Y., Peralta Soler, A., Apodaca, G. L., Harper, J. F., Zheng, Y., and Rajasekaran, A. K. (2001) Na,K-ATPase Activity Is Required for Formation of Tight Junctions, Desmosomes, and Induction of Polarity in Epithelial Cells. **12**, 3717-3732
6. Rajasekaran, S. A., Hu, J., Gopal, J., Gallemore, R., Ryazantsev, S., Bok, D., and Rajasekaran, A. K. (2003) Na,K-ATPase inhibition alters tight junction structure and permeability in human retinal pigment epithelial cells. *American Journal of Physiology-Cell Physiology* **284**, C1497-C1507
7. Cerejido, M. a. C. R. G. a. S. L. a. L. I. (2012) The Na<sup>+</sup> -K<sup>+</sup> -ATPase as self-adhesion molecule and hormone receptor. *American Journal of Physiology-Cell Physiology* **302**, C473--C481
8. Vilchis-Nestor, C. A. a. R. M. L. a. L. A. a. N. J. G. a. P.-B. T. a. S. L. (2019) Ouabain Enhances Cell-Cell Adhesion Mediated by  $\beta$ 1 Subunits of the Na<sup>+</sup>,K<sup>+</sup>-ATPase in CHO Fibroblasts. *International journal of molecular sciences* **20**
9. Reinhard, L. a. T. H. a. C. M. J. a. N. P. (2013) Na<sup>+</sup>,K<sup>+</sup>-ATPase as a docking station: Protein-protein complexes of the Na<sup>+</sup>,K<sup>+</sup>-ATPase. *Cellular and Molecular Life Sciences* **70**, 205--222
10. Barwe, S. P., Anilkumar, G., Moon, S. Y., Zheng, Y., Whitelegge, J. P., Rajasekaran, S. A., and Rajasekaran, A. K. (2005) Novel Role for Na,K-ATPase in Phosphatidylinositol 3-Kinase Signaling and Suppression of Cell Motility. *Molecular Biology of the Cell* **16**, 1082-1094
11. Haas, M., Wang, H., Tian, J., and Xie, Z. (2002) Src-mediated Inter-receptor Cross-talk between the Na<sup>+</sup>/K<sup>+</sup>-ATPase and the Epidermal Growth Factor Receptor Relays the Signal from Ouabain to Mitogen-activated Protein Kinases. *Journal of Biological Chemistry* **277**, 18694-18702
12. Vagin, O., Dada, L. A., Tokhtaeva, E., and Sachs, G. (2012) The Na-K-ATPase  $\alpha$ 1 $\beta$ 1 heterodimer as a cell adhesion molecule in epithelia. *American Journal of Physiology-Cell Physiology* **302**, C1271-C1281

13. Antonicek, H. a. P. E. a. S. M. (1987) Biochemical and functional characterization of a novel neuron-glia adhesion molecule that is involved in neuronal migration. *The Journal of cell biology* **104**, 1587--1595
14. Hilbers, F. a. K. W. a. I. T. J. a. H. T. H. a. L.-H. K. a. N. P. a. K. H. a. P. H. (2016) Tuning of the Na,K-ATPase by the beta subunit. *Scientific reports* **6**, 20442
15. Peng, L. a. M.-V. P. a. S. K. J. (1997) Isoforms of Na,K-ATPase  $\alpha$  and  $\beta$  Subunits in the Rat Cerebellum and in Granule Cell Cultures. *Journal of Neuroscience* **17**, 3488--3502
16. Clausen, M. V. a. H. F. a. P. H. (2017) The Structure and Function of the Na,K-ATPase Isoforms in Health and Disease. *Frontiers in physiology* **8**, 371
17. Litan, A. a. L. Z. a. T. E. a. K. P. a. V. O. a. L. S. A. (2019) A Functional Interaction Between Na,K-ATPase  $\beta$ 2-Subunit/AMOG and NF2/Merlin Regulates Growth Factor Signaling in Cerebellar Granule Cells. *Molecular Neurobiology*, 1--15
18. Magyar, J. P. a. B. U. a. W. Z. Q. a. H. N. a. A. A. a. W. E. F. a. S. M. (1994) Degeneration of neural cells in the central nervous system of mice deficient in the gene for the adhesion molecule on Glia, the beta 2 subunit of murine Na,K-ATPase. *The Journal of cell biology* **127**, 835--845
19. Vagin, O. a. T. S. a. S. G. (2005) Recombinant addition of N-glycosylation sites to the basolateral Na,K-ATPase beta1 subunit results in its clustering in caveolae and apical sorting in HGT-1 cells. *The Journal of biological chemistry* **280**, 43159--43167
20. Vagin, O. a. T. E. a. S. G. (2006) The role of the beta1 subunit of the Na,K-ATPase and its glycosylation in cell-cell adhesion. *The Journal of biological chemistry* **281**, 39573--39587
21. Vagin, O. a. D. L. A. a. T. E. a. S. G. (2012) The Na-K-ATPase  $\alpha$  $\beta$ <sub>1</sub> heterodimer as a cell adhesion molecule in epithelia. *American journal of physiology. Cell physiology* **302**, C1271--1281
22. Lee, S. J. a. L. A. a. L. Z. a. G. B. a. L. S. a. B. S. P. a. L. S. A. (2015) Na,K-ATPase  $\beta$ <sub>1</sub>-subunit is a target of sonic hedgehog signaling and enhances medulloblastoma tumorigenicity. *Molecular Cancer* **14**, 1--13
23. Romer, J. a. C. T. (2005) Targeting Medulloblastoma: Small-Molecule Inhibitors of the Sonic Hedgehog Pathway as Potential \ldots. *Cancer Research*, 4975--4979
24. Marzban, H. a. (2015) Cellular commitment in the developing cerebellum. *Frontiers in Cellular Neuroscience* **8**, 1--26
25. Litan, A. (2018) Isoform-specific functions of the NA, K-ATPase  $\beta$ <sub>1</sub>- and  $\beta$ <sub>2</sub>-subunits in medulloblastoma cells. *University of Delaware*
26. Schulz, A. a. Z. A. a. M. H. (2014) A neuronal function of the tumor suppressor protein merlin. *Acta Neuropathol Commun* **2**, 82

27. Schulz, A. a. B. S. L. a. N.-K. M. a. J. M. J. a. B. R. a. G. C. a. Z. A. a. S. S. a. H. C. a. M. (2013) Merlin isoform 2 in neurofibromatosis type 2-associated polyneuropathy. *Nature Neuroscience* **16**, 426--433
28. Osawa, H. a. S. C. A. a. R. Y. S. a. K. P. a. R. J. T. (2009) The role of the membrane cytoskeleton cross-linker ezrin in medulloblastoma cells. *Neuro-oncology* **11**, 381--393
29. Michie, K. A. a. B. A. a. R. N. O. a. G. S. C. a. C. P. M. G. (2019) Two Sides of the Coin : Ezrin Radixin Moesin and Merlin Control Membrane Structure and Contact Inhibition. *International journal of molecular sciences* **20**, 1--40
30. Schulz, A. a. G. K. J. a. K. S. a. L. G. a. M. H. a. B. S. L. (2010) Cellular/Molecular Merlin Inhibits Neurite Outgrowth in the CNS.
31. Toledo, A. a. G. E. a. K. K. a. M. H. a. B. S. L. (2018) Neurofibromatosis type 2 tumor suppressor protein is expressed in oligodendrocytes and regulates cell proliferation and process formation. *PLoS ONE* **13**, 1--25
32. Toledo, A. a. L. F. a. D. M. a. M. H. a. S. V. a. B. S. L. (2019) Merlin modulates process outgrowth and synaptogenesis in the cerebellum. *Brain Structure and Function* **224**, 2121--2142
33. Curto, M. a. C. B. K. a. L. D. a. L. C. H. a. M. A. I. (2007) Contact-dependent inhibition of EGFR signaling by Nf2/Merlin. *Journal of Cell Biology* **177**, 893--903
34. Kissil, J. L. a. W. E. W. a. J. K. C. a. E. M. S. a. Y. M. B. a. J. T. (2003) Merlin, the Product of the Nf2 Tumor Suppressor Gene, Is an Inhibitor of the p21-Activated Kinase, Pak1. *Molecular Cell* **12**, 841--849
35. Shaw, R. J., Paez, J. G., Curto, M., Yaktine, A., Pruitt, W. M., Saotome, I., O'Bryan, J. P., Gupta, V., Ratner, N., Der, C. J., Jacks, T., and McClatchey, A. I. (2001) The Nf2 Tumor Suppressor, Merlin, Functions in Rac-Dependent Signaling. *Developmental Cell* **1**, 63-72
36. Houshmandi, S. S., Emnett, R. J., Giovannini, M., and Gutmann, D. H. (2009) The Neurofibromatosis 2 Protein, Merlin, Regulates Glial Cell Growth in an ErbB2- and Src-Dependent Manner. **29**, 1472-1486
37. Bashour, A.-M. a. M. J. J. a. I. W. a. M. M. a. R. N. (2002) The Neurofibromatosis Type 2 Gene Product, merlin, Reverses the F-Actin Cytoskeletal Defects in Primary Human Schwannoma Cells. *Molecular and Cellular Biology* **22**, 1150--1157
38. Smole, Z. a. T. C. R. a. A. K. T. a. D. M. a. G. K. L. a. D. G. a. K. W. (2014) Tumor suppressor NF2/Merlin is a microtubule stabilizer. *Cancer research* **74**, 353--362
39. Totaro, A. a. P. T. a. P. S. (2018) YAP/TAZ upstream signals and downstream responses. *Nature Cell Biology* **20**, 888--899
40. Fernandez-Valle, C. a. T. Y. a. R. J. a. R.-R. A. a. T. A. a. H. E. a. B. J. a. I. J. (2002) Paxillin binds schwannomin and regulates its density-dependent localization and effect on cell morphology. *Nature Genetics* **31**, 354--362

41. Cary, L. A., Klinghoffer, R. A., Sachsenmaier, C., and Cooper, J. A. (2002) Src Catalytic but Not Scaffolding Function Is Needed for Integrin-Regulated Tyrosine Phosphorylation, Cell Migration, and Cell Spreading. *22*, 2427-2440
42. Webb, D. J., Donais, K., Whitmore, L. A., Thomas, S. M., Turner, C. E., Parsons, J. T., and Horwitz, A. F. (2004) FAK–Src signalling through paxillin, ERK and MLCK regulates adhesion disassembly. *Nature Cell Biology* **6**, 154-161
43. Poulikakos, P. I. a. X. G. H. a. G. R. a. J. S. a. J. S. C. a. T. J. R. (2006) Re-expression of the tumor suppressor NF2/merlin inhibits invasiveness in mesothelioma cells and negatively regulates FAK. *Oncogene* **25**, 5960--5968
44. Chiasson-MacKenzie, C. a. M. Z. S. a. B. Q. a. M. B. a. C. J. K. a. M. R. a. J. A. E. a. C. T. a. S. S. (2015) NF2/Merlin mediates contact-dependent inhibition of EGFR mobility and internalization via cortical actomyosin. *Journal of Cell Biology* **211**, 391--405
45. Wolle, D. a. L. S. J. a. L. Z. a. L. A. a. B. S. P. a. L. S. A. (2014) Inhibition of epidermal growth factor signaling by the cardiac glycoside ouabain in medulloblastoma. *Cancer Medicine* **3**, 1146--1158
46. Petrilli, A. M. a. F.-V. C. (2016) Role of Merlin/NF2 Inactivation in Tumor Biology. *Oncogene* **35**, 537--548
47. Sabra, H. a. B. M. a. M. V. a. W.-h. B. a. L. D. a. R. A.-s. a. C. G. a. G. P. a. B. M. R. a. B. (2017)  $\beta$ 1 integrin – dependent Rac/group I PAK signaling mediates YAP activation of Yes-associated protein 1 (YAP1) via NF2/merlin. *Journal of Biological Chemistry* **292**, 19179--19197
48. Furukawa, K. T. a. Y. K. a. S. N. a. O. S. (2017) The Epithelial Circumferential Actin Belt Regulates YAP TAZ through Nucleocytoplasmic Shuttling of Article The Epithelial Circumferential Actin Belt Regulates YAP TAZ through Nucleocytoplasmic Shuttling of Merlin. *CellReports* **20**, 1435--1447
49. Yonemura, S., Wada, Y., Watanabe, T., Nagafuchi, A., and Shibata, M. (2010)  $\alpha$ -Catenin as a tension transducer that induces adherens junction development. *Nature Cell Biology* **12**, 533-542

Appendix A

SUPPLEMENTARY IMAGES

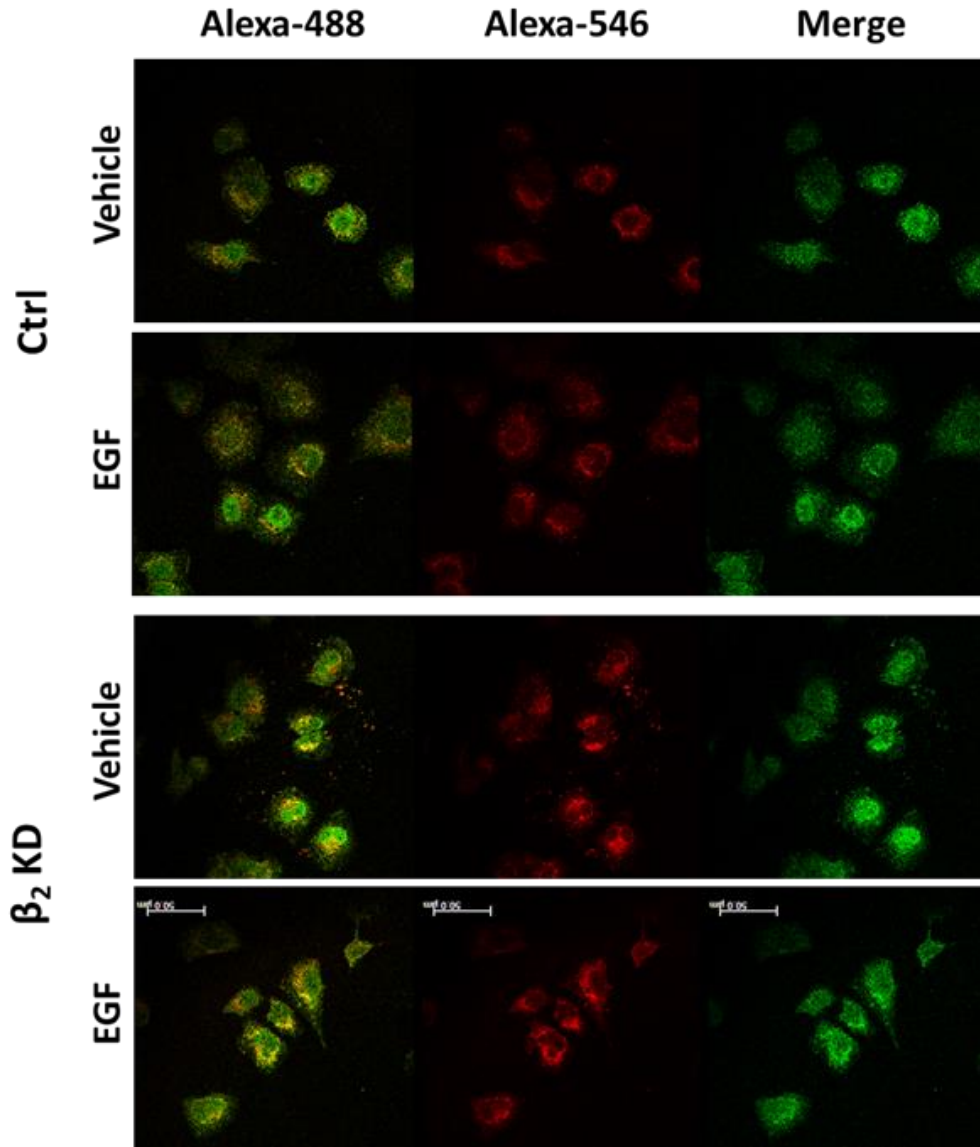


Figure A1.  $\beta_2$  knockdown cells primary control. Fixed Sh  $\beta_2$  Cl. 1 and ShV Cl. 1 cells were incubated in antibody dilution buffer and immunostained with Alexa-488 and Alexa-546 as a primary control. Scale bar: 50  $\mu$ m.

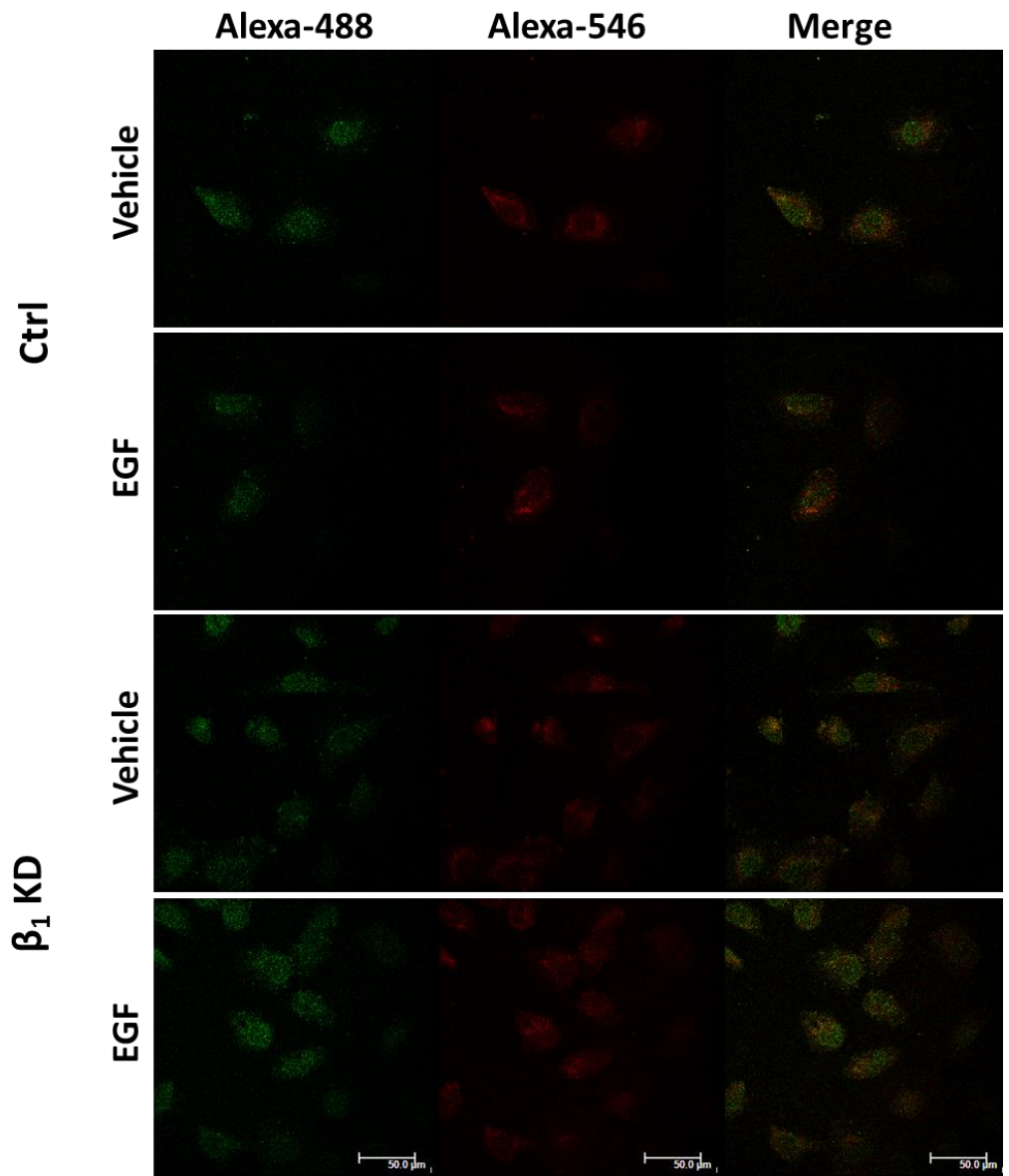


Figure A2.  $\beta_1$  knockdown cells primary control. Fixed Sh  $\beta_1$  Cl. 3 and ShV Cl. 3 cells were incubated in antibody dilution buffer and immunostained with Alexa-488 and Alexa-546 as a primary control. Scale bar: 50  $\mu\text{m}$ .

## Appendix B

### WT AND AMOG<sup>-/-</sup> CEREBELLAR MORPHOLOGY

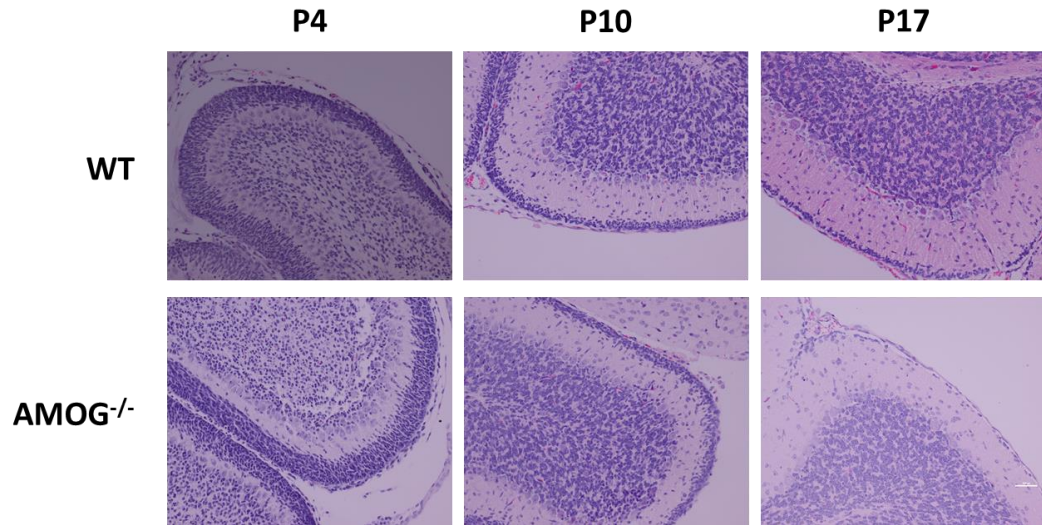


Figure B1. Tissue morphology of WT and AMOG<sup>-/-</sup> cerebellar tissue. Paraffin-embedded tissues were sectioned, stained with hematoxylin and eosin, then imaged with a 20X objective to determine if there were any differences in tissue morphology.

## Appendix C

### PRIMARY CELL CULTURE

Cerebellar tissue was collected from WT P6 pups, when cerebellar granule cells are at the peak of proliferation. The meninges and blood vessels were removed before tissues were digested using a papain dissociation kit (Worthington Biochemical, Lakewood, NJ). Cells were pre-plated to reduce astroglia and seeded in a laminin (5  $\mu\text{g/ml}$ ) and poly-D-lysine (100  $\mu\text{g/ml}$ ) coated 6-well plate inlaid with glass coverslips. Primary cells were maintained with neurobasal medium (0.3125 mM KCl, 12% B27, 1% gentamicin-penicillin-streptavidin) for 72 h before fixation and immunostaining.

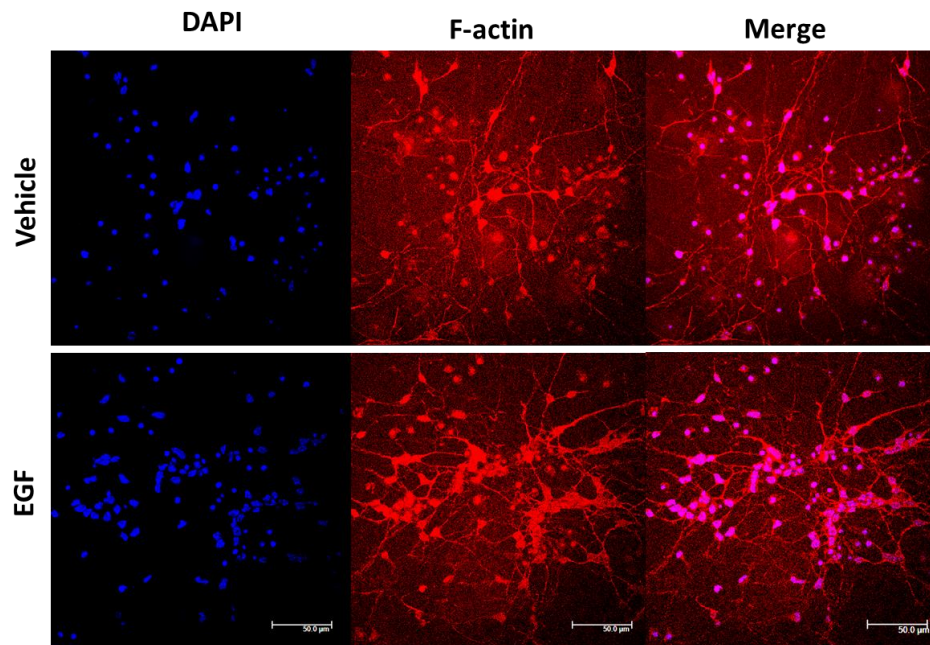


Figure C1. Actin in cerebellar granule progenitor cells. WT P6 granule cell progenitors were treated with 10 ng/ml EGF and stained with phalloidin-594. Scale bar: 50  $\mu\text{m}$ .

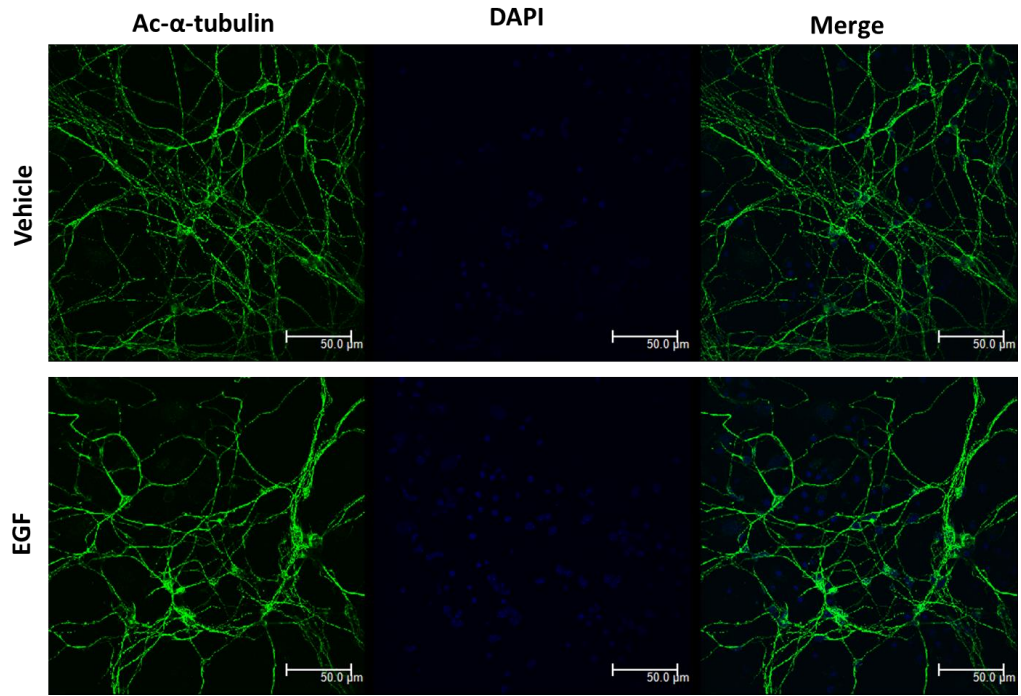


Figure C2. Acetylated  $\alpha$ -tubulin in cerebellar granule progenitor cells. WT P6 granule cell progenitors were treated with 10 ng/ml EGF and stained for acetylated  $\alpha$ -tubulin. Scale bar: 50  $\mu$ m.

## Appendix D

### BETA KNOCKDOWN MEDULLOSPHERES

DAOY ShV Cl. 1, Sh $\beta_2$  Cl. 1, ShV Cl. 3, and Sh $\beta_1$  Cl. 3 were grown in neurobasal medium (0.3125 mM KCl, 2% B27, 1% gentamicin-penicillin-streptavidin) for at least 3 days before imaging.

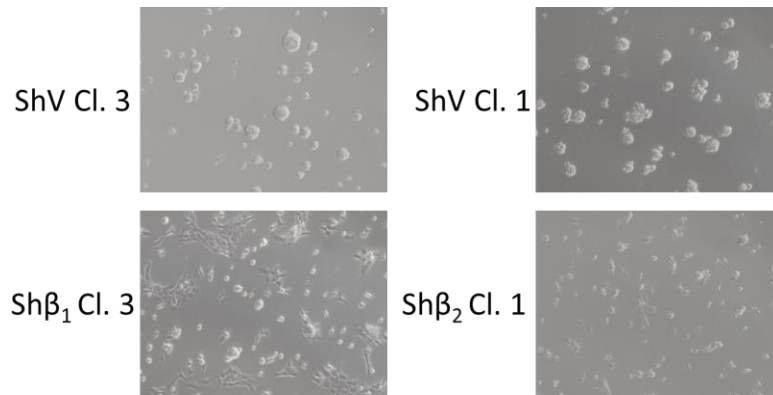


Figure D1. Medullosphere culture of  $\beta$  KD cells. Beta knockdown cells cultured in neurobasal media do not aggregate and adhere to the surface.